Innovation Incubator: LiquidCool Solutions Technical Evaluation

Laboratory Study and Demonstration Results of a Directed-Flow, Liquid Submerged Server for High-Efficiency Data Centers

Eric Kozubal
National Renewable Energy Laboratory

NREL is a national laboratory of the U.S. Department of Energy
Office of Energy Efficiency & Renewable Energy
Operated by the Alliance for Sustainable Energy, LLC

This report is available at no cost from the National Renewable Energy Laboratory (NREL) at www.nrel.gov/publications.

Technical Report
NREL/TP-5500-70459
December 2017

Contract No. DE-AC36-08GO28308

NREL
NATIONAL RENEWABLE ENERGY LABORATORY

Innovation Incubator: LiquidCool Solutions Technical Evaluation

Laboratory Study and Demonstration Results of a Directed-Flow, Liquid Submerged Server for High-Efficiency Data Centers

Eric Kozubal
National Renewable Energy Laboratory

Prepared under Task No. WACC.10105.04.05.01

NREL is a national laboratory of the U.S. Department of Energy
Office of Energy Efficiency & Renewable Energy
Operated by the Alliance for Sustainable Energy, LLC

This report is available at no cost from the National Renewable Energy Laboratory (NREL) at www.nrel.gov/publications.

National Renewable Energy Laboratory
15013 Denver West Parkway
Golden, CO 80401
303-275-3000 • www.nrel.gov

Technical Report
NREL/TP-5500-70459
December 2017

Contract No. DE-AC36-08GO28308

NOTICE

This report is available at no cost from the National Renewable Energy Laboratory (NREL) at www.nrel.gov/publications.

Available electronically at SciTech Connect http:/www.osti.gov/scitech

Available for a processing fee to U.S. Department of Energy and its contractors, in paper, from:

U.S. Department of Energy
Office of Scientific and Technical Information
P.O. Box 62
Oak Ridge, TN 37831-0062
OSTI http://www.osti.gov
Phone: 865.576.8401
Fax: 865.576.5728
Email: reports@osti.gov

Available for sale to the public, in paper, from:

U.S. Department of Commerce
National Technical Information Service
5301 Shawnee Road
Alexandria, VA 22312
NTIS http://www.ntis.gov
Phone: 800.553.6847 or 703.605.6000
Fax: 703.605.6900
Email: orders@ntis.gov

Cover Photos by Dennis Schroeder: (left to right) NREL 26173, NREL 18302, NREL 19758, NREL 29642, NREL 19795.
NREL prints on paper that contains recycled content.

Preface

This work was supported by the Wells Fargo Innovation Incubator (IN^2), a program and platform supporting innovative technologies and innovators. IN^2 is positioned to help companies think about their end customer, providing technical assistance that leverages the capabilities, facilities, equipment, and the deep expertise that exists at the National Renewable Energy Laboratory (NREL), as well as the buildings portfolio of Wells Fargo to help companies de-risk technologies and ease their path to market adoption and deployment. For more information, visit http://in2ecosystem.com/.

Acknowledgments

The author would like to recognize the following efforts and people for their assistance in this project:

- The IN^2 Program for funding the project through a competitive selection process
- David Roe, Rick Tufty, Daryl Lautenschlager, Harsh Patel, Herb Zien, and the rest of the LiquidCool Solutions staff for supporting the project with dedication and indispensable knowledge
- Lucas Phillips who assisted in the test apparatus design, assembly, and installation of the liquid submerged server system at both the Thermal Test Facility and at the Energy Systems Integration Facility
- James Shelby who installed the operating systems and Power Thermal Utility software, and created scripts to operate and collect data on the servers
- David Sickinger who provided insight into the operation of liquid cooled data centers and assisted in the experimental design
- Kevin Regimbal who provided guidance and insight to the operation of liquid cooled data centers
- James Shelby and Henry Horsey for their time and dedication configuring the OpenStudio Server software and Ubuntu operating system during the pilot demonstration at the Energy Systems Integration Facility's High-Performance Computing Data Center
- Report reviewers: David Sickinger, Jennifer Scheib, Kate Cheesbrough, Dane Christensen, Shanti Pless, Kim Trenbath, and Otto VanGeet
- Roger Lyman, Stephen Bigbee, and all other personnel from Intel Corporation who provided Power Thermal Utility software support and data analysis insight.

The IN^2 Program would like to thank the following organizations for supporting the project by donating components and materials used in the LiquidCool Solutions liquid submerged server system:

- Intel Corporation for providing Xeon processors
- Micron Technology for providing server memory
- DSI Ventures, Inc., for providing the dielectric coolant.

List of Acronyms

AVX	advanced vector extensions
CDU	cooling distribution unit
SCMH	standard cubic meters per hour
CMH	cubic meters per hour
CPU	central processing unit
DIMM	dual in-line memory modules
DOE	U.S. Department of Energy
ERW	energy recovery water
ESIF	Energy Systems Integration Facility
HVAC	heating, ventilating, and air conditioning
HPC	high-performance computing
IN^2	Wells Fargo Innovation Incubator
LCS	LiquidCool Solutions
LSS	liquid submerged server
NREL	National Renewable Energy Laboratory
OS Server	OpenStudio server
PDU	power distribution unit
PTU	Power Thermal Utility
TDP	thermal design power

Executive Summary

LiquidCool Solutions (LCS) has developed a liquid submerged server (LSS) technology that changes the way computer electronics are cooled. The technology provides an option to cool electronics by the direct contact flow of dielectric fluid (coolant) into a sealed enclosure housing all the electronics of a single server. The intimate dielectric fluid contact with electronics improves the effectiveness of heat removal from the electronics. The LSS technology has the following advantages over traditional air-cooled server systems:

1. Maintains a small difference between central processing unit (CPU) and memory temperatures and inlet coolant temperature, allowing for:
    A. Use of higher temperature coolant
    B. Higher temperature heat recovery
    C. Ability to maintain lower electronic temperatures
2. Eliminates the parasitic cooling energy used by fans
3. Lowers capital and energy costs in a building that contains a data center because the heat removed from the servers can:
    A. More effectively be rejected to ambient conditions using lower cost systems
    B. Be re-used effectively as a heating source for the building.

The LSS shown in Figure ES-1 is encased in a liquid-tight aluminum housing and was outfitted with two windows such that the internal electronics and motherboard are visible.

Figure ES-1. An LSS in liquid-tight aluminum housing
Photo by Dennis Schroeder, NREL

Figure ES-2 shows a depiction of how the coolant flows through the liquid submerged server. Coolant is introduced from a no-spill fitting at the lower right (blue arrow). The coolant is then directed toward the two copper heat spreaders attached to the CPUs. It then flows out of the heat spreader and around the remaining server electronics. Finally, the coolant is collected in a manifold situated at the front end (left) of the server and directed to the top-right no-spill fitting, where it exits the server (red arrow).

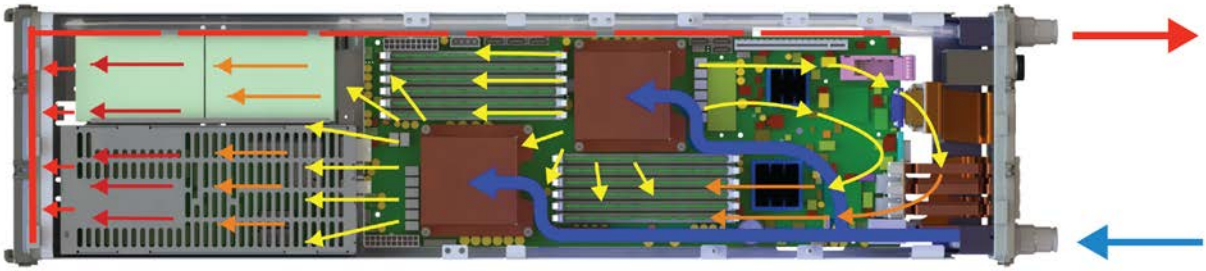

Figure ES-2. Depiction of liquid flow path through the LSS.
Graphic by Steve Shafer, LCS and Marjorie Schott, NREL

Because of the technology's potential, the IN^2 Program selected LCS to participate in the program to further develop and accelerate commercialization of its cooling technology. The IN^2 Program, funded by the Wells Fargo Foundation and co-administered by NREL on behalf of the U.S. Department of Energy (DOE), is a $30-million program supporting innovative technologies and innovators.

Pursuant to the IN^2 award, the project was set up into two phases. In phase one, an experimental LSS system comprising eight high-performance servers (the specifications are shown under "HVAC Laboratory and Equipment Setup") and the associated liquid cooling system was installed at NREL's Advanced Heating, Ventilating, and Air Conditioning Systems Laboratory in Golden, Colorado. The subsequent experiments characterized the liquid cooling performance of the LSS system. It also provided LCS with verification and design assistance of a water-side temperature control system that interfaces the LSS dielectric fluid cooling system with a data center's facility energy recovery water system. Phase two used the laboratory data to design a pilot LSS system rack and demonstrate it at NREL's Energy Systems Integration Facility (ESIF) data center.

Phase One: Laboratory Experiments and Analysis of the LSS System

Figure ES-3 shows the eight servers installed and tested at the HVAC Laboratory. Experiments done under phase one show that the LSS paired with the LL800 cooling distribution unit (CDU) can be operated to maintain acceptable electronic temperatures. Most liquid cooling approaches involve a CDU, which interfaces with the facility cooling system and provides cooling liquid at the appropriate temperature, pressure, and chemistry for the information technology equipment.[1] Experiments revealed an operational envelope of dielectric flow rate and inlet temperature (to the LSSs) to maintain the following requirements:

[1] Taken from https://hpc.nrel.gov/datacenter/energy-efficient-data-center-cooling-system

1. CPU temperatures below 100°C
2. Memory temperatures below 85°C
3. Balance of motherboard and supporting electronics submersed in coolant less than 60°C.

Figure ES-3. Eight servers instrumented at NREL's Advanced HVAC Systems Laboratory in Golden, Colorado
Photo by Eric Kozubal, NREL

Intel's Power Thermal Utility (PTU) software was used to drive the CPUs and memory from 50% to 100% of typical computing processing levels with associated increase in power consumption (subsequently referred to as [percent] % PTU test in this report). It was also used to drive the CPUs up to thermal design power (TDP) conditions using Intel's advanced vector extensions (AVX) test. This latter test, which is atypical of normal operation, is useful in determining the performance of the LSS and CDU system under the most extreme thermal load conditions. The software also records the power and temperatures of the CPUs and memory.

Experiments show that the acceptable maximum inlet coolant temperature is from 50°C to 54°C as dielectric fluid flow increases from 8.2 kg/min to 14.5 kg/min (1.0 kg/min to 1.8 kg/min per server). Maintaining acceptable outlet coolant temperature below 60°C during TDP tests was found to be the limiting factor in determining inlet coolant temperature. This temperature was chosen as the safe level for the motherboard electronics, which are the last components in contact with the coolant before it exits the LSS. The maximum CPU temperature rise above inlet coolant temperature is between 34°C and 27°C as the coolant flow ramps from 1.0 kg/min up to 1.8 kg/min per server. The maximum CPU temperature is expected to be less than 84°C. Under more typical (lower power) CPU computing loads (such as that when the PTU test is set at 50% to 100%), the CPU temperatures are expected to be less than 72°C.

Under peak memory power use conditions, which occurred during 100% tests, the memory temperatures are maintained below an 8°C rise above outlet coolant temperature. Thus, the

highest memory temperature is expected to be 68°C, which is safely below the memory temperature requirement.

The LSSs were also characterized to determine the level of liquid heat recovery by the water feeding the CDU and how much was "lost" to the air surrounding the test equipment. Liquid heat recovery efficiency was measured using calorimetry techniques in which the total water-side heat recovery was measured as a percentage of electric power into the servers. The calorimeter's air temperature was a constant 25.6°C for these tests, while the inlet coolant temperature was adjusted. It was found that computing load, which affects electric power into the servers, and temperature of the outlet dielectric fluid affected the water heat recovery efficiency. Heat recovery efficiency was measured between 90% and 95% (Figure ES-4), with higher efficiency at higher computing load and lower temperature difference between outlet dielectric fluid and the surrounding air. The latter affects the heat transfer between surface of the LSS case and the surrounding air. Because this experiment was relatively small in comparison to a full-rack system, the percent heat loss to the surrounding air is expected to reduce as more servers are added to a single rack. Heat recovery can be improved further using strategic thermal insulation around the servers, CDU, and high-temperature hoses.

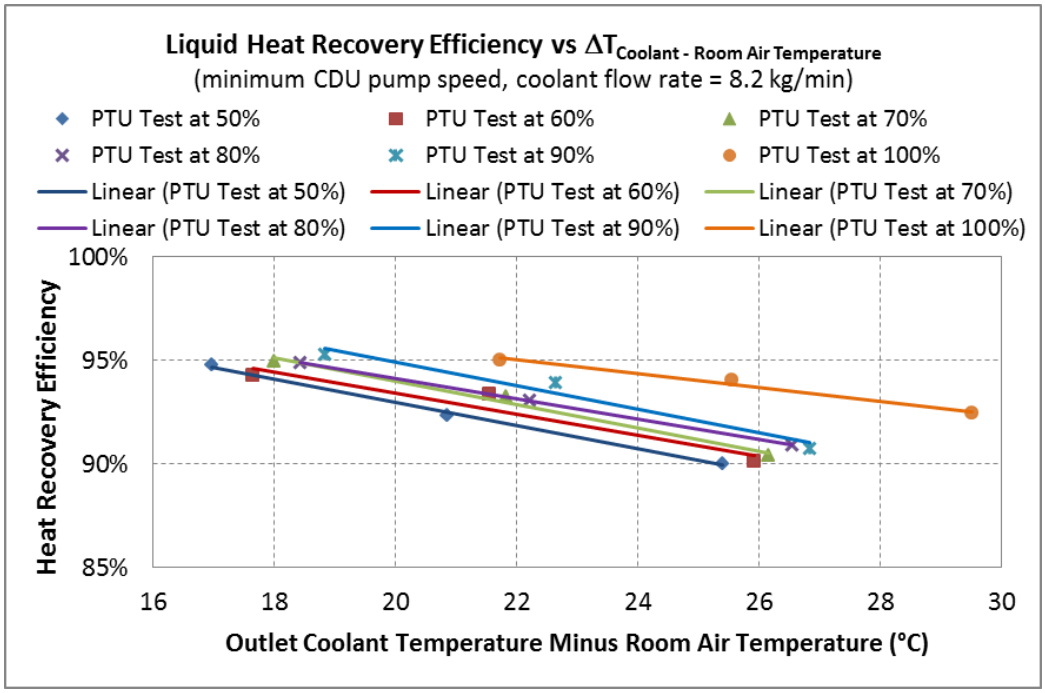

Figure ES-4. Heat effiiciency versus delta coolant/room air temperature

The LL800 CDU maintained 49°C outlet water temperature while limiting the coolant temperature to 60°C. However, future CDU designs should increase the heat exchanger size and effectiveness such that the outlet water temperature approaches 60°C. The current CDU's internal heat exchanger was designed to cool eight–16 servers at lower water inlet temperature and flow. To efficiently reject heat using a dry cooler (radiator) during a warm day or to a building's heating system, the water temperature and flow rate through the CDU will increase. To operate under these conditions, the effectiveness of the CDU's internal heat exchanger should be increased to operate above 80% during these higher flow conditions. Eighty percent

effectiveness ensures that the water temperature is sufficiently hot enough to reject heat to hot ambient conditions or to be effectively reused in building heating systems. Alternatively, the dielectric fluid can be directed to a fluid to air heat exchanger if this system arrangement can maintain acceptable fluid cleanliness and pressure at the servers.

Phase Two: Pilot Demonstration at the ESIF's Liquid Cooled Data Center

The objectives of demonstrating the LCS technology at NREL's High-Performance Computing (HPC) Data Center[2] were to:

1. Determine a system design suitable for acceptable performance in a liquid cooled data center
2. Determine operational characteristics in a data center environment and verify acceptable thermal performance
3. Record and report observations of the LSS system.

The LSS system was modified to operate at the ESIF's liquid cooled data center, which uses an energy recovery water loop to cool the computing resources in the data center. Most of the cooling is provided to NREL's Peregrine HPC and other system resources which require approximately 1 MW of thermal cooling as of August 2017. This same coolant loop, which supplies water at a temperature between 18.3°C and 23.9°C, was tapped to cool the pilot LSS system. Figure ES-5 shows the LCS server rack installed in the data center.

The rack design, informed by testing in phase one, included the necessary upgrades to:

1. Monitor server health and shut down the system's servers upon detection of breaching high-temperature limits
2. Control water return temperature back to the data center at 49°C in order to maintain coolant temperatures at less than 60°C
3. Provide safe operational features to control hazards associated with high-temperature operation and the possibility of dielectric coolant leaks.

The demonstration was split into two parts, commissioning and operation. The commissioning process (Sept. 28 through Oct. 11, 2016) was used to verify safe operation and had three steps:

1. Simulation of step change to high computational load
2. Simulation of master CDU shut down
3. Long-term simulation of high computational load.

These steps showed that the system maintained CPU and component temperatures within their thermal design limits while providing 49°C energy recovery water temperature back to the data center's facility. However, the redundant CDU design (in a master/slave configuration) was unable to seamlessly transfer cooling requirements from the master CDU to the slave CDU during commissioning. This was not detrimental to the demonstration, as the monitoring system

[2] https://www.nrel.gov/computational-science/facilities.html

successfully operates to safely shut down the servers. Fixing this issue is a matter of operating two pumps simultaneously such that upon failure of one pump (by mechanical or electrical fault), the second pump seamlessly increases speed. The system was allowed to operate despite this flaw because the use case is not critically reliant on server up-time.

After the commissioning was completed, the system's operation was transferred to NREL's commercial buildings staff for their research purposes. To satisfy their initial resource requirements, they installed OpenStudio® Server software[3] on three (of the eight) server nodes to support the research objectives of NREL's commercial and residential buildings program.[4] During heavy compute requirements, the server CPU temperatures were monitored as an indicator of operation. To verify successful operation, the server cooling system was monitored during a nine-hour period of peak computing, during which the system maintained all CPU temperatures at or below 77°C. No thermal anomalies were recorded by the monitoring system during this operational period through September 2017. NREL's buildings group will continue to operate the LSSs through September 2018 with all eight nodes eventually loaded with OpenStudio Server software.

[3] https://www.openstudio.net/
[4] https://www.nrel.gov/buildings/

Figure ES-5. Left: Eight-server rack from the back. Right: Eight-server rack from the front.
Photos by Dennis Schroeder, NREL

Table of Contents

List of Figures

List of Tables

1 Introduction

LiquidCool Solutions (LCS) has developed liquid submerged server (LSS) technology that changes the way computer electronics are cooled. The technology provides an option to cool electronics by the direct contact flow of dielectric fluid (coolant) into a sealed enclosure housing all the electronics of a single server. The intimate dielectric fluid contact with electronics improves the effectiveness of heat removal from the electronics. The LSS technology has the following advantages over traditional air-cooled server systems:

1. Maintains a small difference between central processing unit (CPU) and memory temperatures and inlet coolant temperature, allowing for:
    A. Use of higher temperature coolant
    a. Higher temperature heat recovery
    B. Ability to maintain lower electronic temperatures.
2. Eliminates the parasitic cooling energy used by fans
3. Lower capital and energy costs in a building that contains a data center because the heat removed from the servers can:
    A. More effectively be rejected to ambient conditions using lower cost systems
    B. Be re-used effectively as a heating source for the building.

The LSS shown in Figure 1 is encased in a liquid-tight aluminum housing and was also outfitted with two windows such that the internal electronics and motherboard are visible.

Figure 1. An LSS in liquid-tight aluminum housing
Photo by Dennis Schroeder, National Renewable Energy Laboratory (NREL)

Figure 2 shows a depiction of how the coolant flows through the LSS. Coolant is introduced from a no-spill fitting at the lower right (blue arrow). The coolant is then directed toward the two copper heat spreaders attached to the CPUs. It then flows out of the heat spreader and around the remaining server electronics. Finally, the coolant is collected in a manifold situated at the front end (left) of the server and directed to the top-right no-spill fitting, where it exits the server (red arrow).

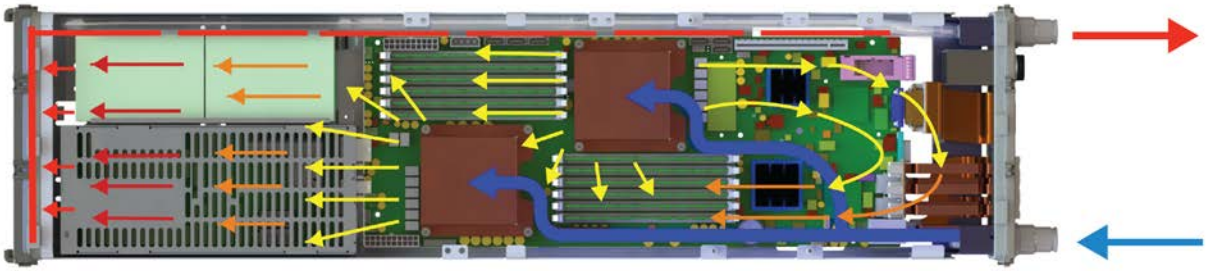

Figure 2. Depiction of liquid flow path through the LSS
Graphic by Steve Shafer, LCS and Marjorie Schott, NREL

Because of the technology's potential, the Wells Fargo Innovation Incubator (IN^2) program selected LCS to participate in the program to further develop and accelerate commercialization of its cooling technology. The IN^2 Program, funded by the Wells Fargo Foundation and co-administered by NREL on behalf of the U.S. Department of Energy (DOE), is a $30-million program supporting innovative technologies and innovators.

Pursuant to the IN^2 award, the project was set up into two phases. In phase one, an experimental LSS system comprising eight high-performance servers (the specifications are shown under the "HVAC Laboratory and Equipment Setup" section) and the associated liquid cooling system was installed at NREL's Advanced Heating, Ventilation, and Air-Conditioning (HVAC) Systems Laboratory in Golden, Colorado. The subsequent experiments characterized the liquid cooling performance of the LSS system. It also provided LCS with verification and design assistance of a water-side temperature control system that interfaces the LSS dielectric fluid cooling system with a data center's facility water system. Phase two used the laboratory data to design a pilot LSS system rack and demonstrate it at NREL's Energy Systems Integration Facility (ESIF) data center.

Figure 3. Eight servers instrumented at NREL's Advanced HVAC Systems Laboratory in Golden, Colorado (left) and eight servers installed at NREL's ESIF data center in Golden, Colorado (right)
Photos by Eric Kozubal and Dennis Schroeder, NREL

2 Phase One: Laboratory Experiments and Analysis of the LSS System

2.1 Phase One Objectives

The objectives of the first phase of the project were twofold: (1) verify that the LSS system design maintains acceptable operating temperatures and parameters of the CPUs, memory, and other electronics submerged in the coolant; and (2) characterize the heat recovery effectiveness of the liquid coolant and the opportunity to recover heat energy at a useful fluid temperature.

The system was installed into a test facility that measures all the electric power and heat flows in and out of the LSS system. This experimental setup provided a platform to verify proper cooling of the electronics, such as the CPUs, memory, and motherboard. The experiments were designed to feed back the necessary data to determine the operational space within which the newly designed LSS system could safely operate. Experiments were also intended to reveal the effectiveness of the liquid system in its ability to collect the thermal heat and reject it outside of a data center.

2.2 HVAC Laboratory and Equipment Setup

The test system is a high-performance computing platform comprising eight LSS servers and were configured with one head node and seven processing nodes. The total combined computing load of the servers is approximately 3,000 W. Each server was configured with the following components.

1. Supermicro X10DRT-LIBQ motherboard
2. Dual Intel Xeon E5-2690 V3 CPUs
3. 64-GB DDR4 2133 MT/s Memory (8 x 8-GB dual in-line memory modules [DIMMs])
4. 2X Intel 530 Series 120-GB Solid State Drives
5. I/O ports:
    A. 2X SFP+ (Head node), 1X SFP+ (Processing nodes)
    B. 2X 1-GB Ethernet
    C. 2X USB 2.0
    D. 1X BMC (IPMI 2.0).

The LSS system delivered for testing included the following system components:

1. One LL800 8-kW liquid-to-liquid cooling distribution unit (CDU) with a water temperature control valve
2. Explorer ruggedized portable electronics rack
3. Mounting hardware, manifolds, hoses, and power cords for the servers and CDU
4. Tripp Lite PDUMH30HV 2U 30-A 208-V power distribution unit (PDU)
5. Drain/fill station for removing and adding coolant to the servers.

NREL's Advanced HVAC Systems Laboratory (Figure 4) is a facility that has the following high-level capabilities.

1. Eight air stream pairs (inlet and outlet) that can be controlled as follows:
    A. Air flow rate from 0 to 8,500 cubic meters per hour (CMH)
    B. Air temperature from -5°C to 150°C
    C. Air dew point temperature from -20°C to 50°C.
2. 20 tons of chilled water from -5°C to 35°C
3. 1.4-Million-Btu boiler system up to 110°C
4. National Instruments-based data acquisition and control system that measures and controls both laboratory and test article functions
5. High accuracy instruments to measure electric power, flow rates, and moist air properties, which leads to measured energy balance error of thermal-electric systems to better than ±5%.

Figure 4. Wide-angle view of NREL's Advanced HVAC Systems Laboratory in Golden, Colorado
Photo by Warren Gretz, NREL

To use the provided system from LCS, a water-side experimental apparatus had to be constructed to mimic a data center cooling system. The process flow diagram in Figure 5 shows the liquid flows (water and dielectric fluid) and the measurement instrumentation installed. The sensors, pumps, and valves were connected to the data acquisition system to control the parameters of the experiments and measure the outputs. This liquid-side test setup is flexible because the water temperature is controlled by modulating chilled water entering the coolant loop. The water flow rate through the CDU was controlled by the variable-speed water pump. The CDU flow rate was controlled using the LCS software interface and CDU onboard controller. Most liquid cooling

approaches involve a CDU, which interfaces with the facility cooling system and provides cooling liquid at the appropriate temperature, pressure, and chemistry for the information technology equipment.[5] In the figure, the "chilled water apparatus" was designed to mimic a facility cooling system, but with higher flexibility to change water temperature and flow rate.

[5] Taken from https://hpc.nrel.gov/datacenter/energy-efficient-data-center-cooling-system

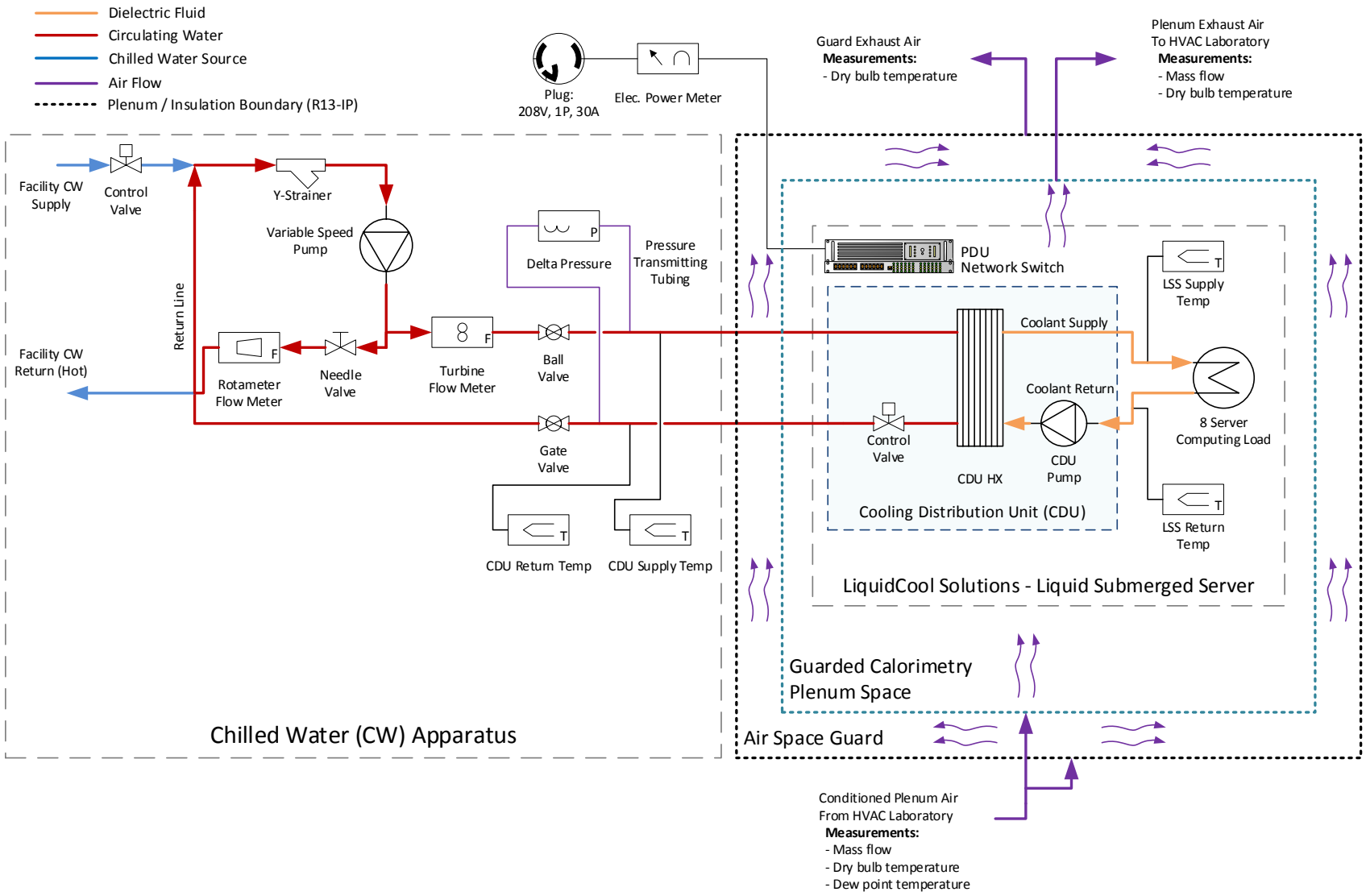

Figure 5. Process schematic showing fluid flows and sensors used to measure electrical and thermal power flows

The water-side heat rate was determined using a volumetric flow measurement and temperature measurements configured with six Type T thermocouples: three thermocouples on each of the CDU's entering and leaving water streams. The typical water-side heat rate uncertainty was less than ±3%. However, under high water flow conditions (i.e., low water-side temperature rise), the uncertainty was found to be up to ±5%. Because it was impractical to install flow metering on the dielectric fluid (coolant) stream, this flow rate was inferred from the dielectric fluid temperatures and heat rate through the CDU heat exchanger. The dielectric fluid temperatures were measured using Type T thermocouples that were surface mounted to the metal connectors close to the CDU connections. The surface mounts were insulated to prevent heat loss and provide an accurate fluid temperature measurement.

Power measurements (shown at the top/middle of Figure 5) into the LSS system were obtained with a single source electric power meter with ±0.5% of full-scale measurement uncertainty. Full scale was set to 4,000 W, resulting in a maximum ±20 W power measurement uncertainty.

The systems above were used to measure liquid heat rate in and out of the LSS test setup. Figure 6 shows the LSS system installed in a guarded calorimeter at NREL's HVAC facility. The calorimeter incorporates the water-side heat rate measurements and captures the air-side heat loss from the LSS system (also shown in Figure 5). The inner chamber's air temperature was controlled using the HVAC laboratory's air-conditioning system. The calorimeter is supplied with the following streams from the HVAC laboratory:

1. 208-Volt, single-phase power for the LSS system
2. A water coolant inlet and outlet high flow stream
3. A water coolant return stream that exits the CDU
4. An inlet and outlet air flow to the inner chamber to maintain ambient temperature surroundings of the LSS system
5. An inlet and outlet air flow to the outer chamber plenum at the same temperature delivered to the inner chamber; this is used as a guard against heat flow through the inner chamber walls.

The result is a complete balance of input electrical power measurement that can be compared to the air and water-side heat rate. This energy balance error was measured to be less than ±6% during all experiments, with average values of about ±3%. Maintaining steady balance (near 0%) ensures the experiment is at steady state and that the measurements and resulting calculations of thermal and electrical power are operating correctly. Steady state was typically achieved about 30 minutes after changing test conditions, or changing server computing level, fluid flow rates, and fluid temperatures.

Figure 7 shows the inlet air vents supplied to the inner chamber of the calorimeter. This air is controlled by the HVAC laboratory's fan system and conditioned to the correct temperature and humidity. Inlet air temperature is measured with Type T thermocouples at the vents. Inlet air humidity is measured with a chilled mirror, dew-point hygrometer.

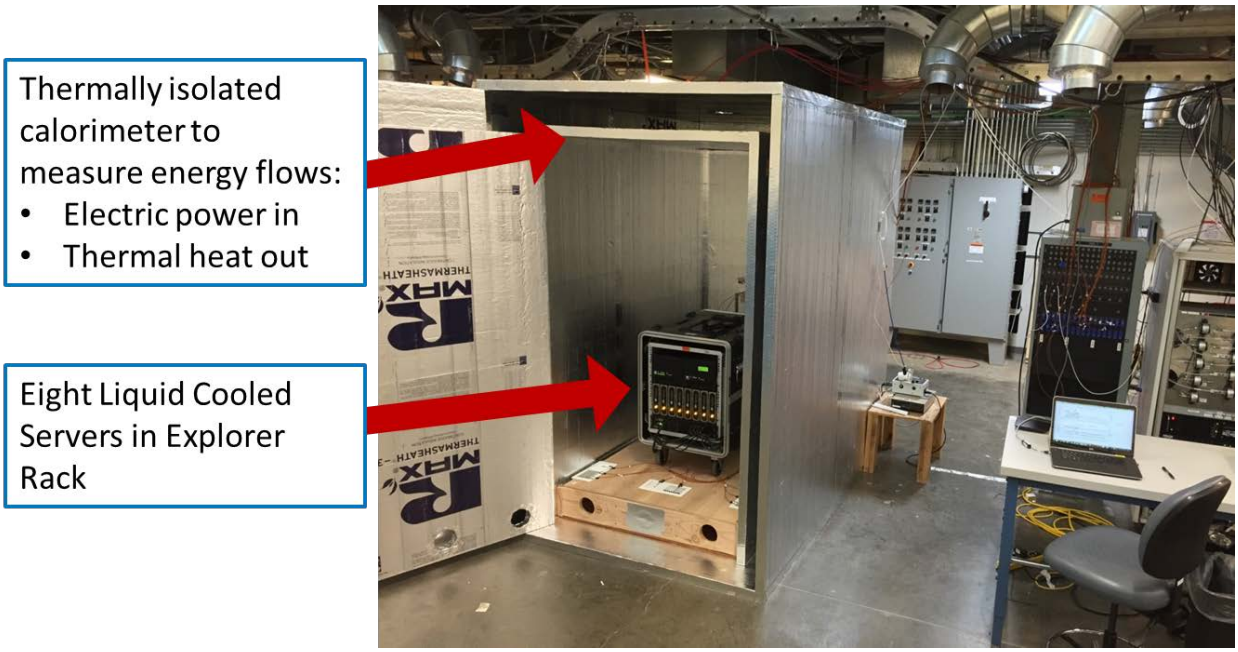

Figure 6. Eight LSS servers in compact rack, sitting inside a guarded calorimeter at NREL's Advanced HVAC Systems Laboratory
Photo by Eric Kozubal, NREL

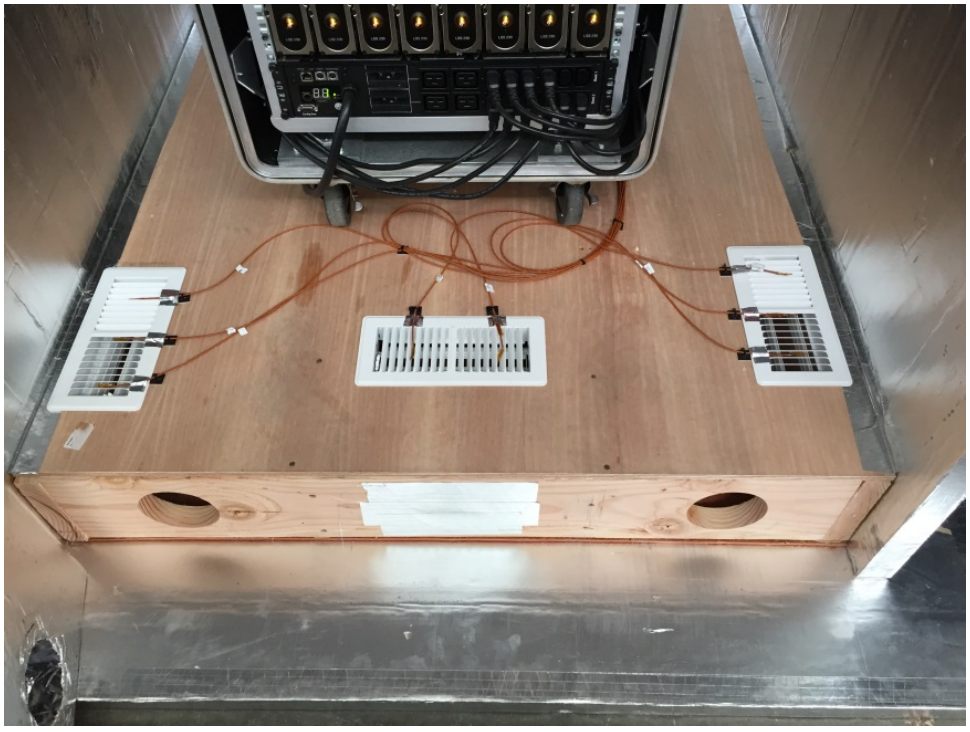

Figure 7. Chamber inlet air vents (white) with thermocouple temperature measurements
Photo by Eric Kozubal, NREL

Figure 8 shows the back of the calorimeter and the air ducts in and out of it. The inlet duct supplies about 200 CMH into the calorimeter. The air is split into two 100-CMH streams; one

stream is directed into the inner air chamber and the other is directed into the guarded plenum space around the inner chamber. The second air stream, being at the same temperature as the first, guards against heat loss out of the inner chamber, thus limiting heat transfer through the inner chamber walls. The maximum air heat loss is estimated to be less than 40 W. The outlet air stream (100 CMH) temperature is measured with Type T thermocouples. The air-side heat rate was determined by the mass flow rate of air and the air temperature rise through the room air chamber. Air-side heat rate uncertainty was determined to be less than ±20 W for all experiments.

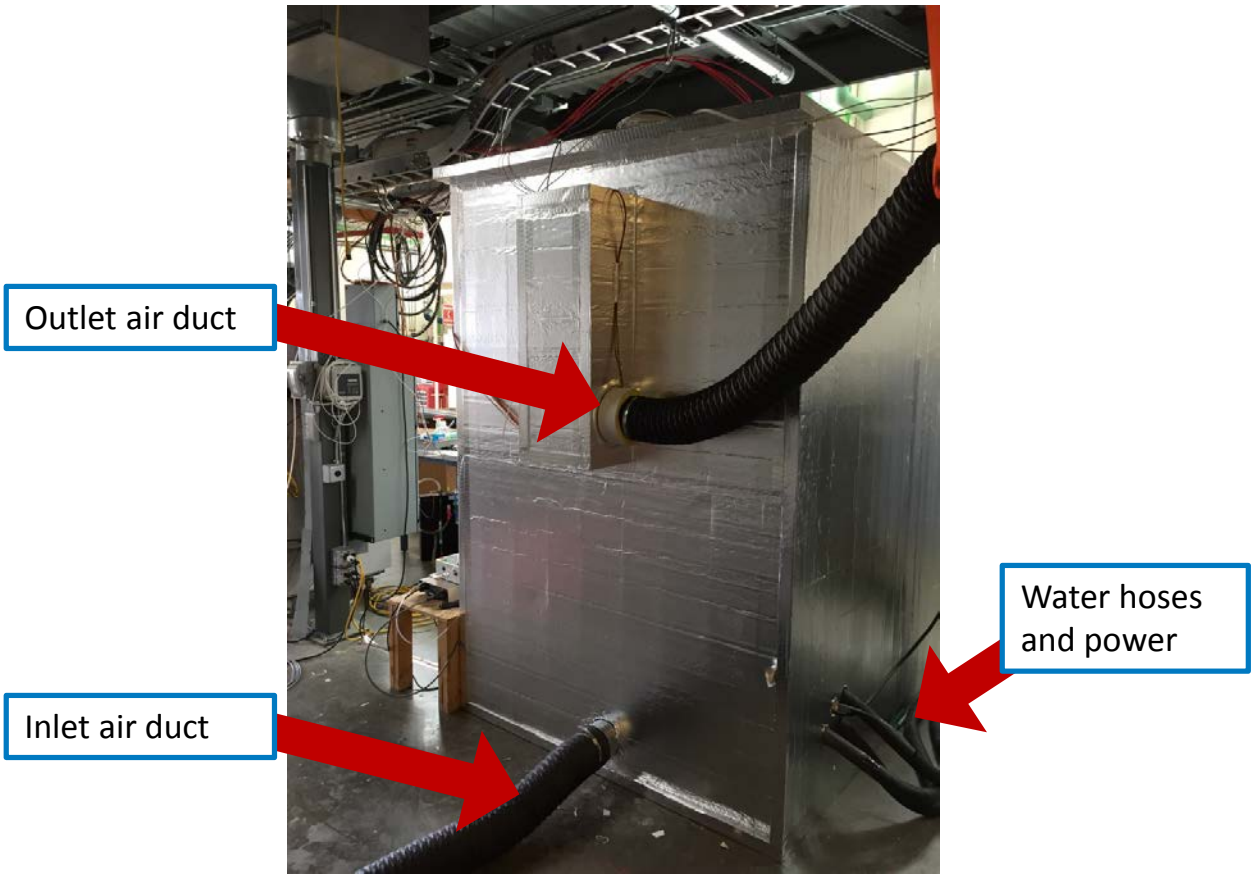

Figure 8. Rear of calorimeter showing inner chamber inlet/outlet air ducts, water hoses, and power cord

Photo by Eric Kozubal, NREL

Figure 9 shows the system with the doors to the calorimeter closed and the LSS system under test. To the right side is the hydronic components assembled onto a cart.

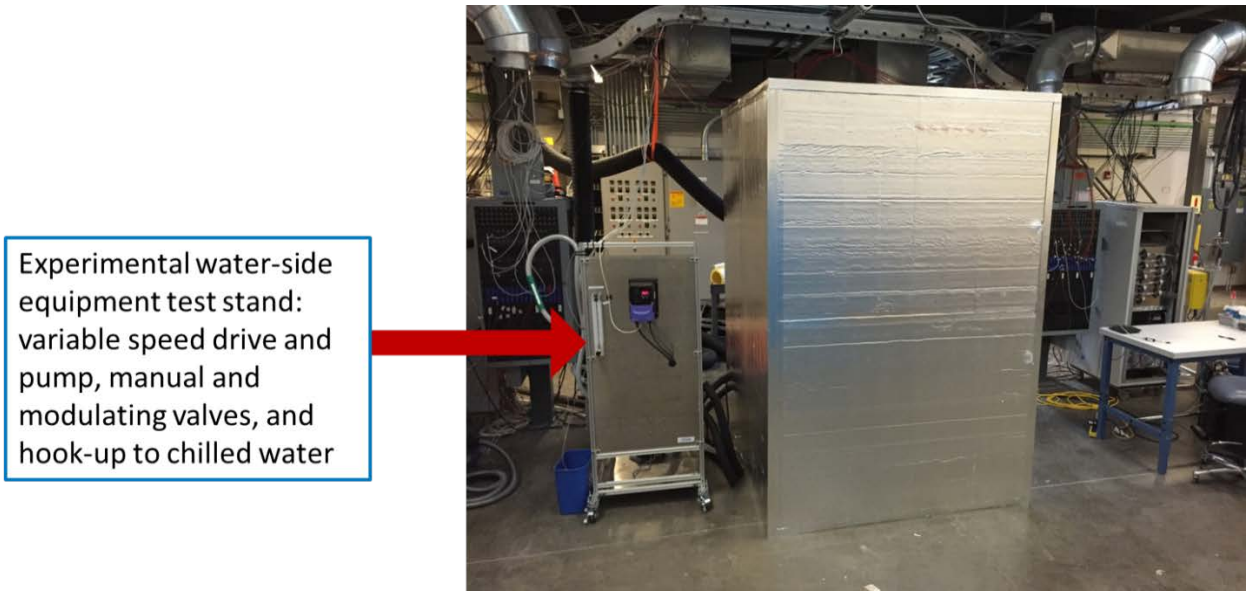

Figure 9. Calorimeter and pump station under test
Photo by Eric Kozubal, NREL

The computer systems were installed with CentOS Version 6 and configured in a cluster of one head node and seven standard compute nodes. Intel's Power Thermal Utility (PTU) software was installed on all nodes. Seven modes of software control were used, and all nodes ran the same software settings for each test. For six tests, the PTU software was set to core processing levels of 50%, 60%, 70%, 80%, 90%, and 100%. The memory read-write test was enabled during these tests to stress the 8 DIMMs in each server. To test thermal design power (TDP), the core advanced vector extensions (AVX) test was used. This last test uses Intel's AVX instructions that stress the CPU to its maximum thermal capability by operating the CPU up to its TDP. According the Intel's white paper, "If you are a thermal engineer, the processor TDP specification is very important because your thermal solution (fans, heat sink, etc.) must be able to dissipate the rated TDP value."[6]

The PTU software logs the readings from on-board or on-die sensors for CPU power, core temperatures (two per core and 24 total per CPU) and the physical temperature of the CPU. Upon inspection of the data, the physical temperature was found to be approximately the same as (i.e., within 1°C of) the maximum of the core temperatures. The software also logs onboard memory temperatures. The maximum memory temperature of each memory bank (0 and 1), each containing four DIMMS, was used as the memory temperature for each test.

The experiments were designed to deliver different water recovery temperatures and flow rates as well as dielectric fluid temperatures and flow rates. The matrix of experiments is listed in Appendix A: Experiment Matrix. Each experiment was intended to be taken at steady state. Steady-state time-series data were recorded for a minimum of 15 minutes for each test. The measured parameters were then averaged into single numbers that were used as the value for each test. These values were then used as "measured values" from which analysis was performed

[6] Intel White Paper, *Measuring Processor Power* (Intel, April 2011). https://www.intel.com/content/dam/doc/white-paper/resources-xeon-measuring-processor-power-paper.pdf

and calculations were derived. For each test, a spreadsheet of all the values was populated with measured results for that test and calculations were performed (see Appendix B: Example of Detailed Output and Calculations). The data were analyzed to show aggregated performance of all the servers, CPUs, and memory measurements. Aggregated performance was then used to create the trend plots described in the Phase One Results and Data Section.

2.3 Phase One Results and Data

The data shown in this report are intended to determine operational characteristics of the LSS system and from those determine bounds for safe operation of the servers. The server's CPUs are self-protecting against thermal damage, as the processors begin to lower their processing speed (or frequency) in response to the CPU's core temperature sensor. This throttling of CPU speed occurs at 100°C, thus maintaining CPU core temperatures safely below 100°C is required. The DIMM memory high limit temperature is 85°C according to the manufacturer (Micron). Lastly, the exiting coolant temperature was limited to 60°C because the remaining motherboard electronics are a mixture of many types of electronic components, of which the lowest temperature specification becomes the limiting factor. The coolant exiting the CPU heat spreader then flows around the remaining motherboard electronics. Therefore, the exiting coolant temperature is conservatively assumed to be in contact with the most temperature-sensitive electronic components. Because of these constraints, the experiments were designed to map the operational space of the coolant inlet temperature and flow rate in which the above constraints are satisfied.

Figure 10 shows the individual CPU power (as reported by the PTU software) and total input power to all the servers as a function of the PTU test setting for all tests performed (see Appendix C). Because there were eight servers with 16 total CPUs, the data going forward are shown in terms of average, minimum, and maximum for all 16 CPUs. Note that during the AVX tests, the measured power for the CPUs has a nearly zero-watt difference between maximum and minimum of all the CPUs. According to Intel's PTU documentation, the AVX test will exceed the processors TDP. These power readings are all at the processor's TDP (135 W). A similar plot for measured memory power is shown in Figure 11. In this case, the memory power is the power for each of two memory banks in each server. Each memory bank contains four DIMMs. These results later guide the results of fluid temperature vs. electrical power input. The temperature of the respective electronic component (CPU or memory DIMM) is determined by how much electric power it consumes.

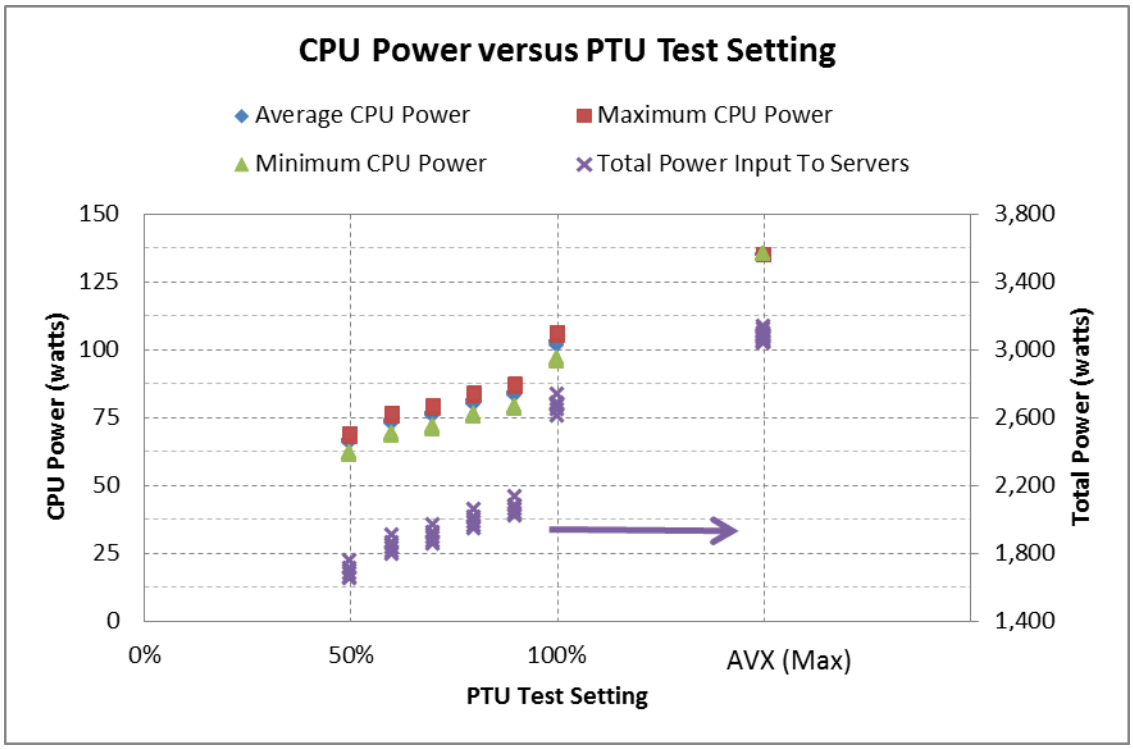

Figure 10. CPU power versus PTU test setting

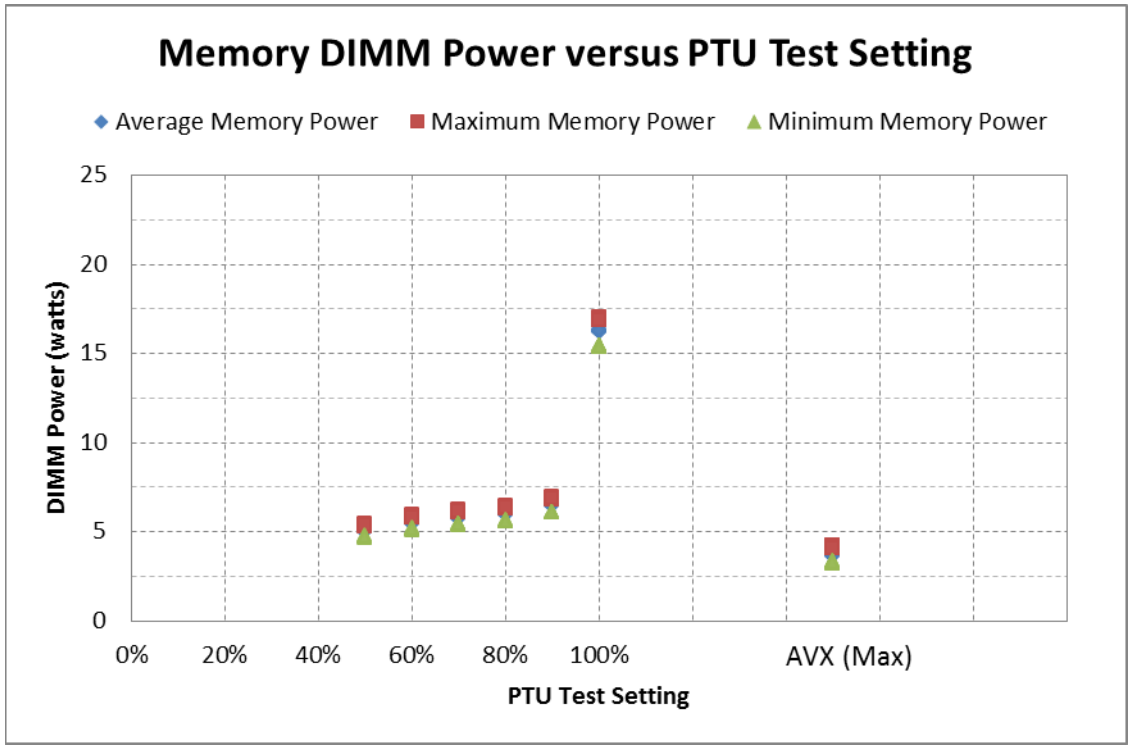

Figure 11. Memory DIMM power versus PTU test setting

Figure 12 shows the temperature rise of the coolant above the inlet temperature into the servers as a function of the average CPU power input to the servers. From this, one can see the maximum temperature rise is about 9.3°C, 5.8°C, and 5.2°C for coolant flow rates from 8.2

kg/min, 12.7 kg/min, and 14.5 kg/min respectively. This equates to an average of 1.02 kg/min, 1.60 kg/min, and 1.81 kg/min flow to each individual server. The relative scatter for the 8.2 kg/min group is due to the change in heat recovery efficiency (which is discussed below). This flow rate range correlates to the minimum and maximum flow settings for the CDU. To maintain a maximum 60°C coolant outlet temperature, these values should be subtracted from 60°C to come to the maximum allowable inlet coolant temperature. The current version of the CDU software will ramp the CDU pump to maintain a maximum outlet coolant temperature. Thus, it is possible for the water-side flow rate controller to maintain a 54°C or lower inlet coolant temperature. However, it is desirable to operate the CDU pump at its minimum speed to save pump power (as described later and shown in Figure 23). Thus, maintaining the inlet coolant at or below 50°C is desired to maintain a less than 60°C exit coolant temperature. This maintains motherboard and power supply electronic components immersed in coolant at less than 60°C.

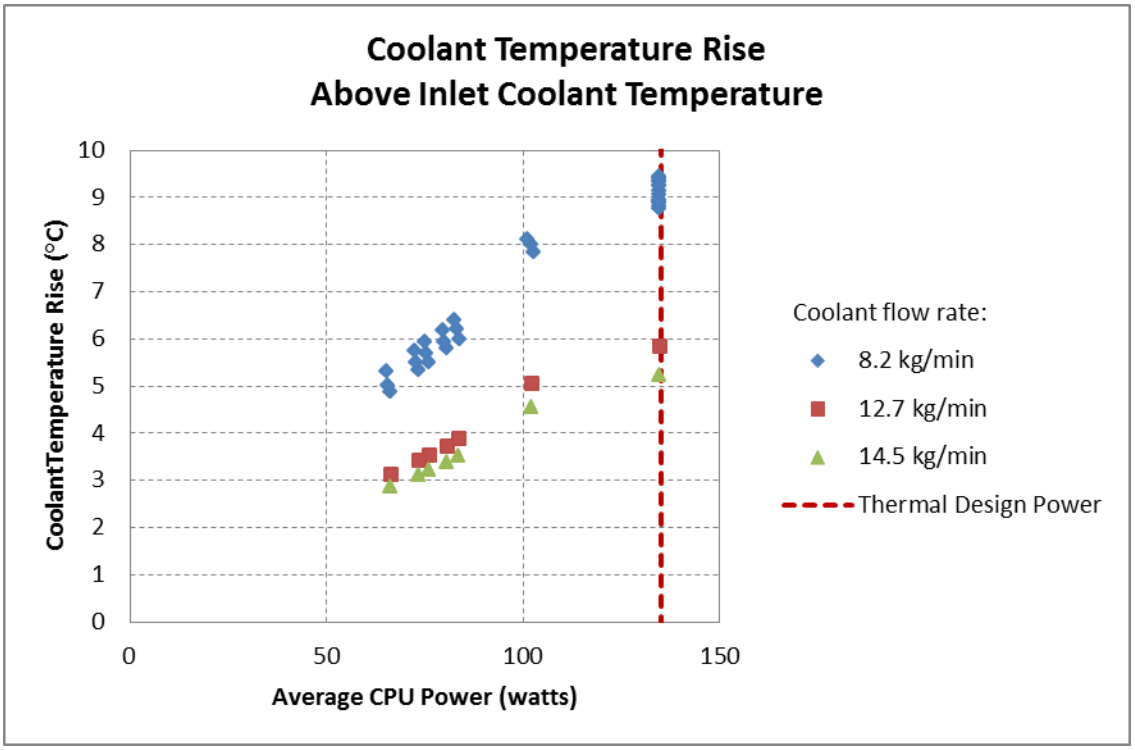

Figure 12. Coolant temperature rise above inlet coolant temperature

Figure 13 through Figure 15 show the CPU temperature rise above the inlet coolant temperature as a function of average CPU power. PTU tests from 50% to 100% setting are shown as the cluster of points at and below about 105 W. Under typical maximum computing conditions (PTU set at 100%), the highest CPU core temperature rise is shown at 8.2 kg/min coolant flow. Therefore, the maximum processor core temperatures would normally be at 22°C above the inlet coolant temperature, which in turn would be about 72°C during 100% operation. During maximum operation (using the AVX tests), which deliberately drives the CPUs up to TDP, the maximum CPU temperature rise is about 34°C. According to Intel's application engineering, this mode is atypical for most applications and the test is intended as a tool for determining thermal headroom. Therefore, the maximum expected core temperature will be 84°C with 50°C inlet coolant temperature. Furthermore, under maximum CDU flow rate (14.5 kg/min), the CPU temperature rise is reduced to 27°C. This correlates to a maximum CPU core temperature of

about 81°C at the maximum inlet coolant temperature of 54°C. In either case represented above, the CPU core temperature are maintained sufficiently below the 100°C maximum temperature at which the CPUs begin to self-protect or throttle.

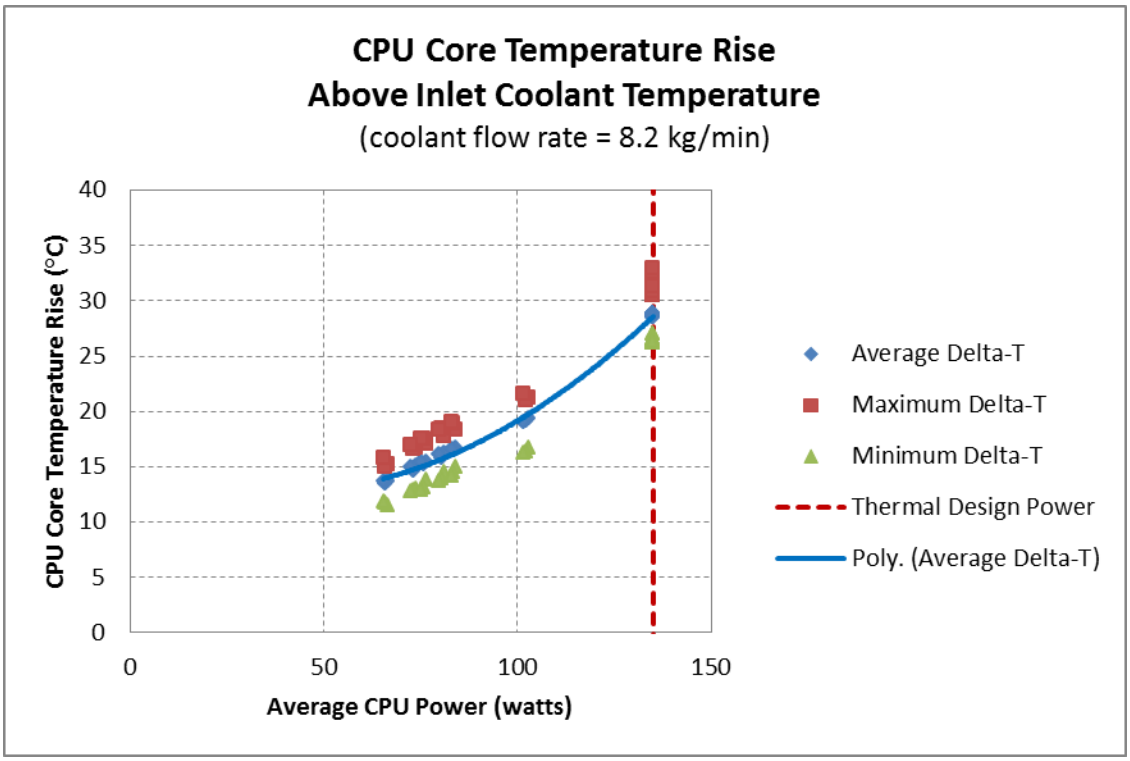

Figure 13. CPU core temperature rise above inlet coolant temperature at 8.2 kg/min coolant flow rate

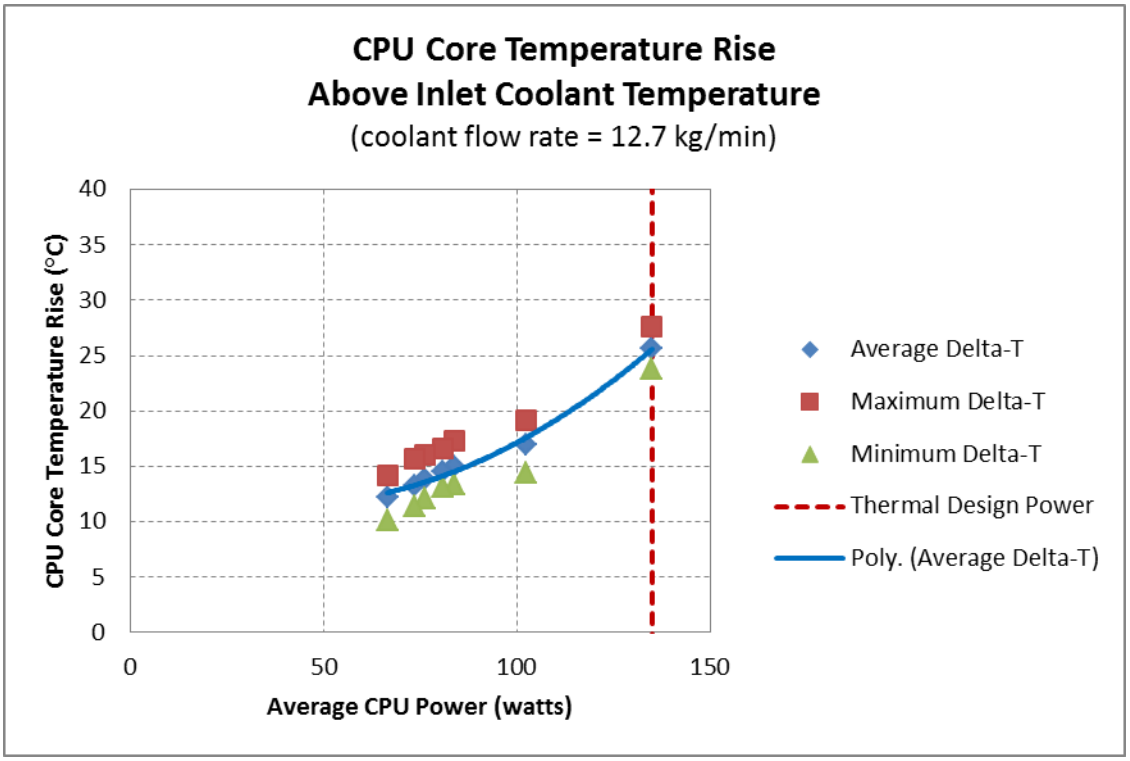

Figure 14. CPU core temperature rise above inlet coolant temperature at 12.7 kg/min coolant flow rate

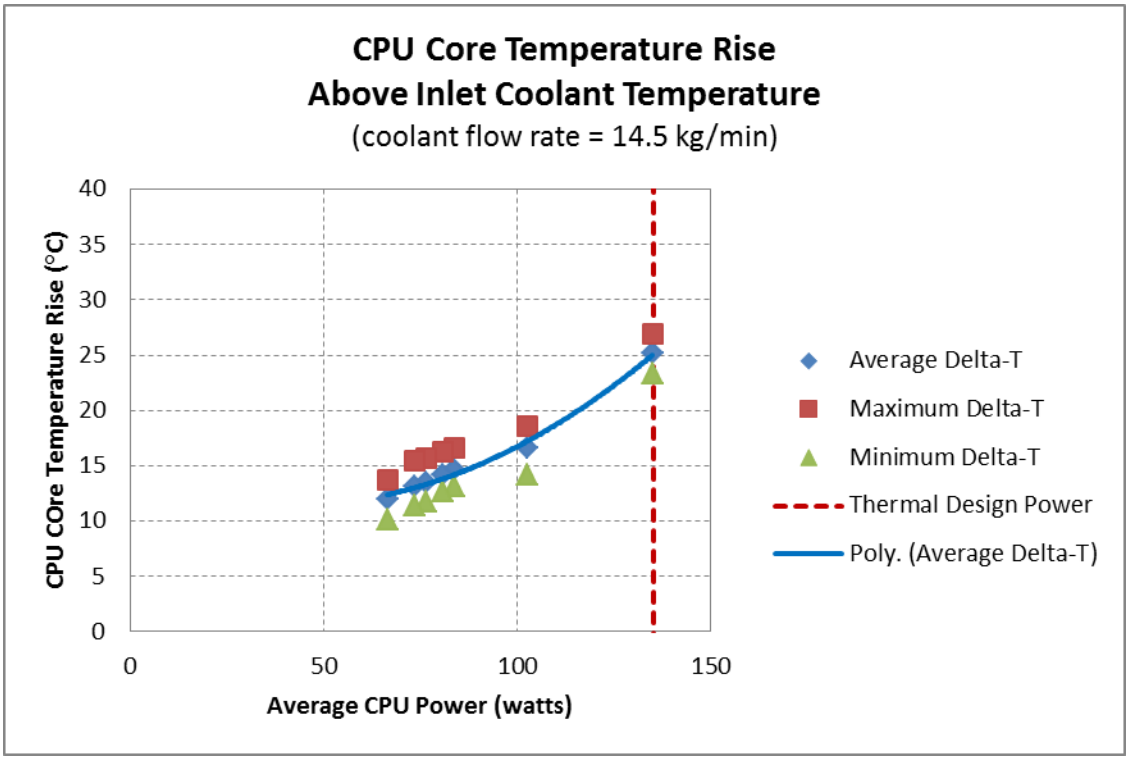

Figure 15. CPU core temperature rise above inlet coolant temperature at 14.5 kg/min coolant flow rate

Figure 16 and Figure 17 show the CPU power draw as measured by the PTU software as a function of CPU temperature and inlet coolant temperature respectively. For the temperature range shown, the power use was measured to increase about 0.14 W/°C for the PTU tests from 50% to 90% and about 0.17 W/°C for the 100% test. The CPU power can also be plotted as a function of the inlet coolant temperature as shown in Figure 17, which shows a power increase of 0.12 W/°C and 0.14 W/°C. This relation of CPU power to temperature is likely the result of increased "leakage power." However, leakage power was not directly measured during these experiments. The data show the relevant energy savings by maintaining a lower CPU temperature. In combination with data from Figure 13 through Figure 15, the LSS system typically maintain less than 20°C core temperature rise above the inlet coolant temperature, thus limiting leakage power to less than about 3.4 W above the thermodynamic limitation (a hypothetical heat sink that cools the CPU down to the inlet coolant temperatures).

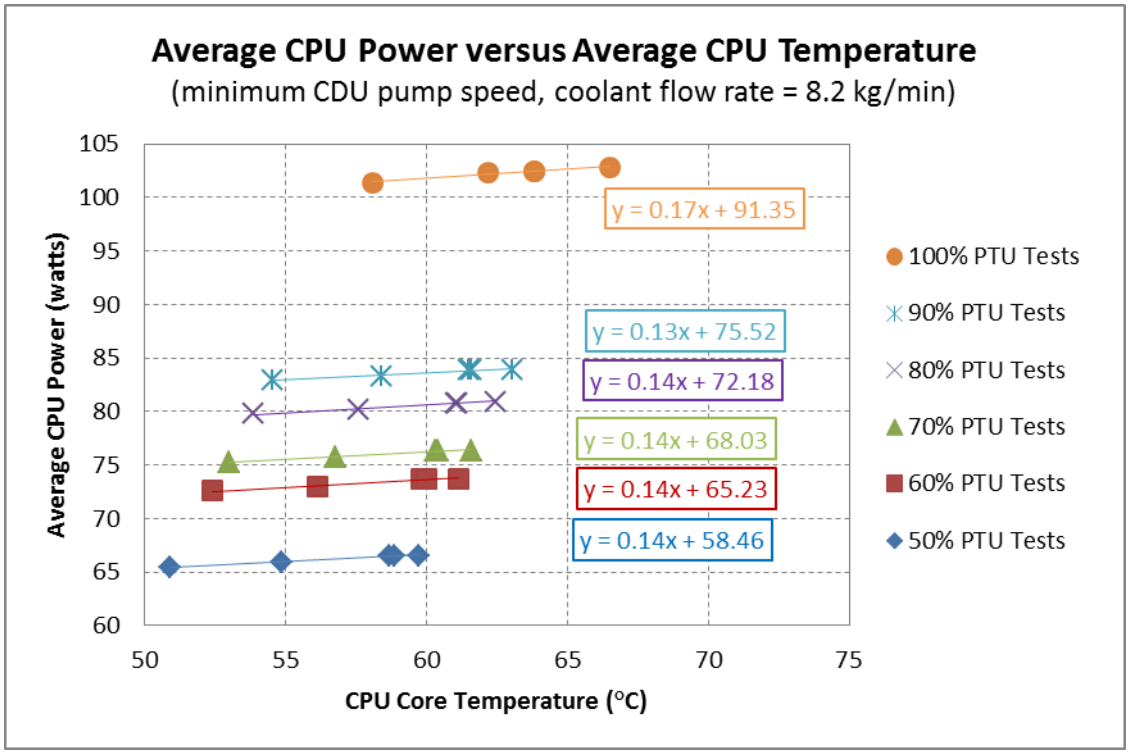

Figure 16. Average CPU power versus average CPU temperature

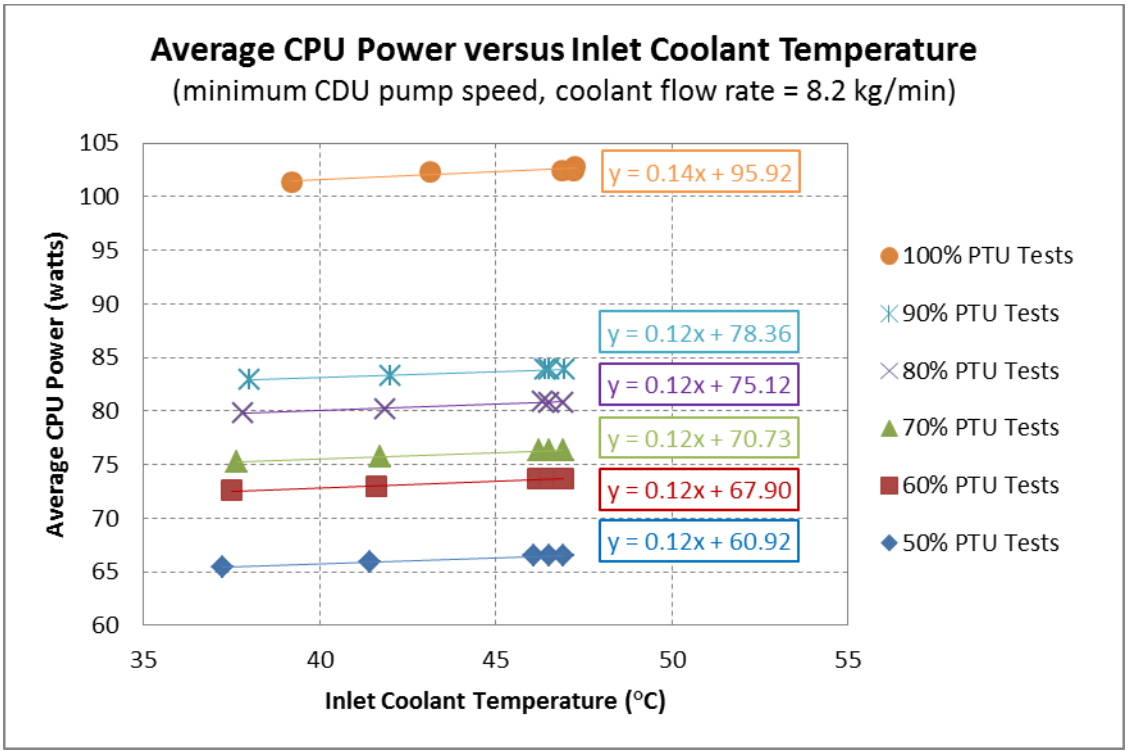

Figure 17. Average CPU power versus inlet coolant temperature

Figure 18 through Figure 20 show the measured memory temperatures for all the tests but broken into three groups of PTU test modes. The reported temperatures for each server are the maximum temperature for all memory DIMMs in a single bank. The system consisted of two memory banks with four DIMMs in each bank. It was found that the temperature rise above outlet coolant temperature shows different trends for each of these three groups. These groups correlate with three distinct memory power levels for each test (Figure 11). The outlet coolant temperature is reported as the independent variable because (1) the memory is most closely thermally coupled with the coolant exiting the CPUs, (2) and because the CPUs represent the majority of the power use (between 62% and 72% of the total server power), the memory experiences coolant closer in temperature to that of the outlet coolant stream. Upon inspection of these results, the memory temperature is seen to be on average about 4°C above the outlet coolant temperature for the 50% to 90% and AVX tests, and it is about 7°C above the outlet coolant temperature for the 100% test. The worst case (maximum) temperature above the outlet coolant temperatures was found to be 8°C. If the outlet coolant temperature is controlled to less than 60°C, the memory should remain at or below 68°C, which is sufficiently below the 85°C maximum temperature for the memory.

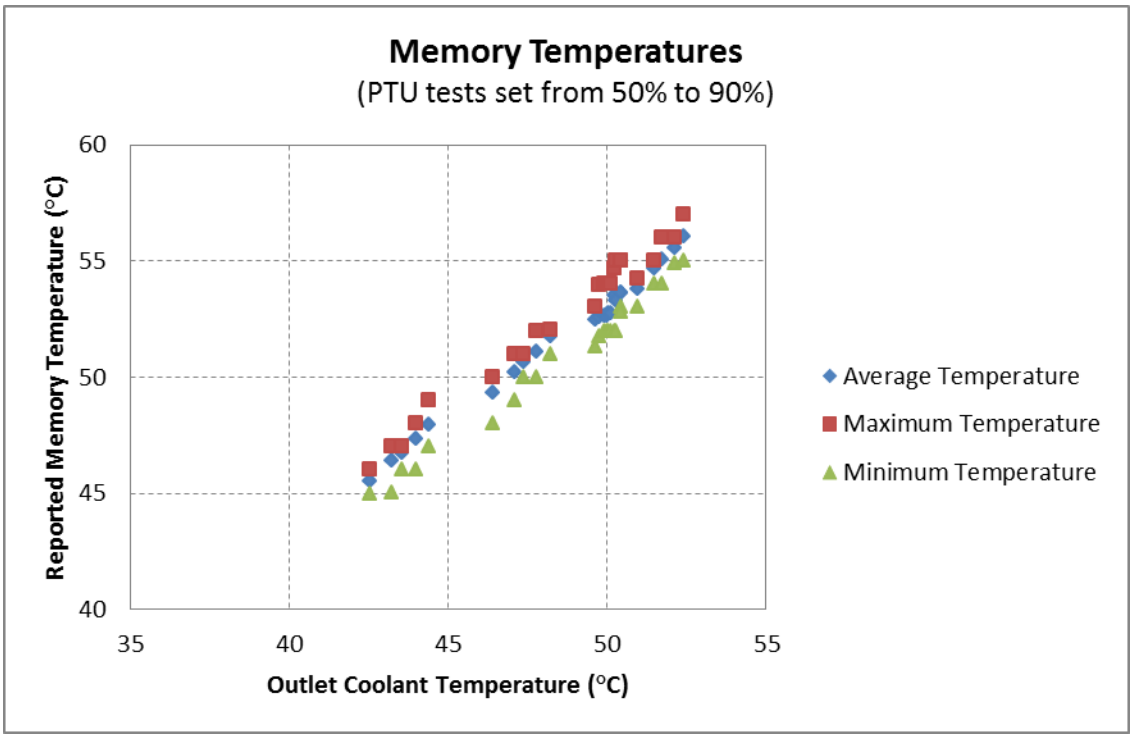

Figure 18. Memory temperature: PTU test set from 50% to 90%

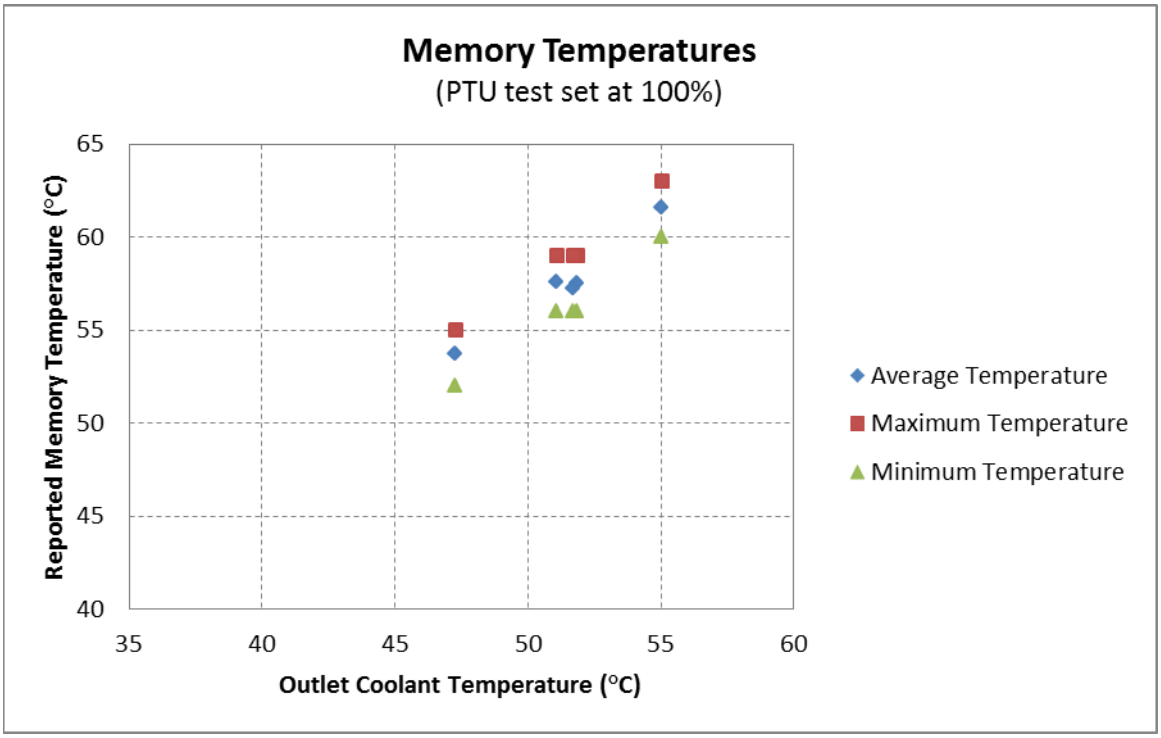

Figure 19. Memory temperature: PTU test set at 100%

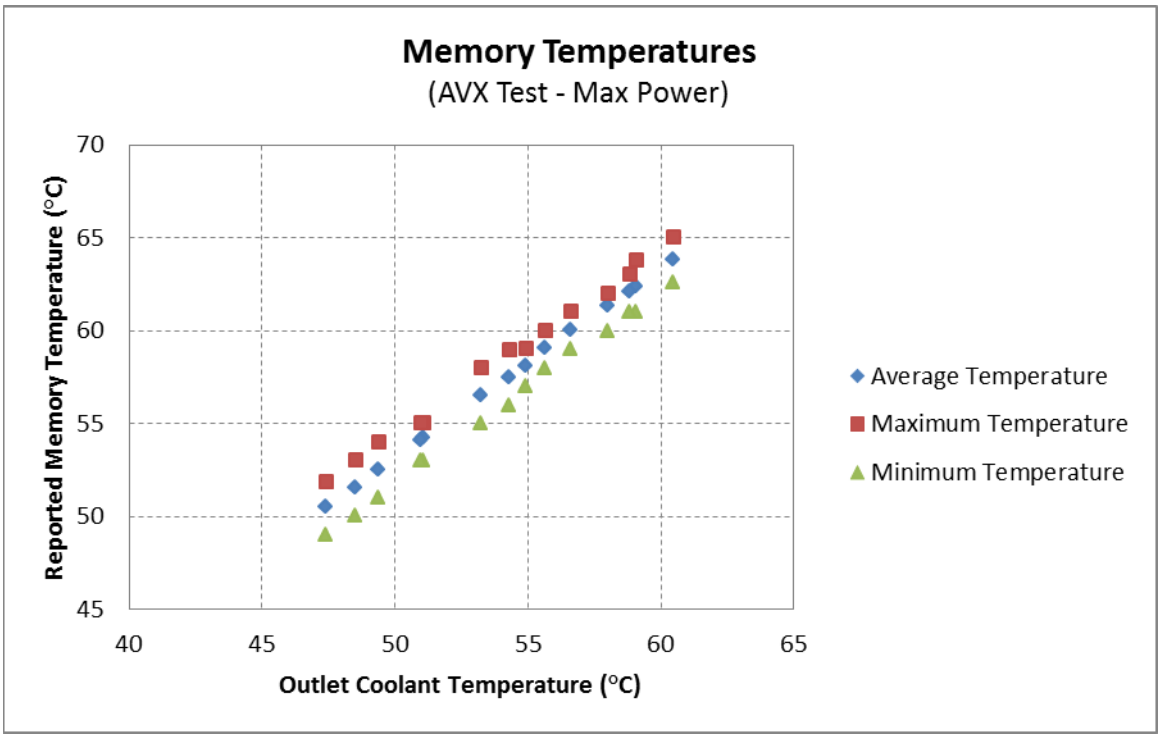

Figure 20. Memory temperature: PTU set to AVX test

Figure 21 and Figure 22 show the liquid heat recovery efficiency for the LSS system, which is defined as follows:

$$Heat\ Recovery\ Efficiency = \frac{Thermal\ Power\ Recovered\ by\ the\ CDU\ (W)}{Electrical\ Power\ to\ Servers\ (W)}$$

Because the outlet coolant temperature and server casing temperature are closely related, the heat recovery efficiency is thus related to the difference in the outlet coolant temperature and the surrounding room air. This temperature difference dictates the heat rejected to the room air and thus cannot be captured by the liquid stream and directed away from the server rack by the CDU. The data show that the liquid heat recovery efficiency increases with the higher computing level and the lower delta temperature. The data show 90% to 95% heat recovery efficiency, meaning that most of the thermal heat is collected by the liquid system rather than expelled to the room air. Increasing the number of servers in a rack will raise the heat recovery efficiency, as the heat loss to the surrounding air will disproportionately decrease because a smaller fraction of server case area is exposed to the ambient air. Furthermore, the test setup had no thermal insulation wrapped around the sides of the servers; increasing server thermal insulation around the servers would also increase heat recovery. The water lines leading up to the servers and the coolant lines from the CDU to the servers were insulated. Therefore, omitting these insulation covers would decrease heat recovery in an actual installation. A potential economical solution is to insulate the system rack on all six sides. In doing so, a designer should also be cognizant of non-server equipment that may be air cooled or have temperature limits that are incompatible with the LSSs. Such equipment should not reside within any thermally insulated volumes of a rack.

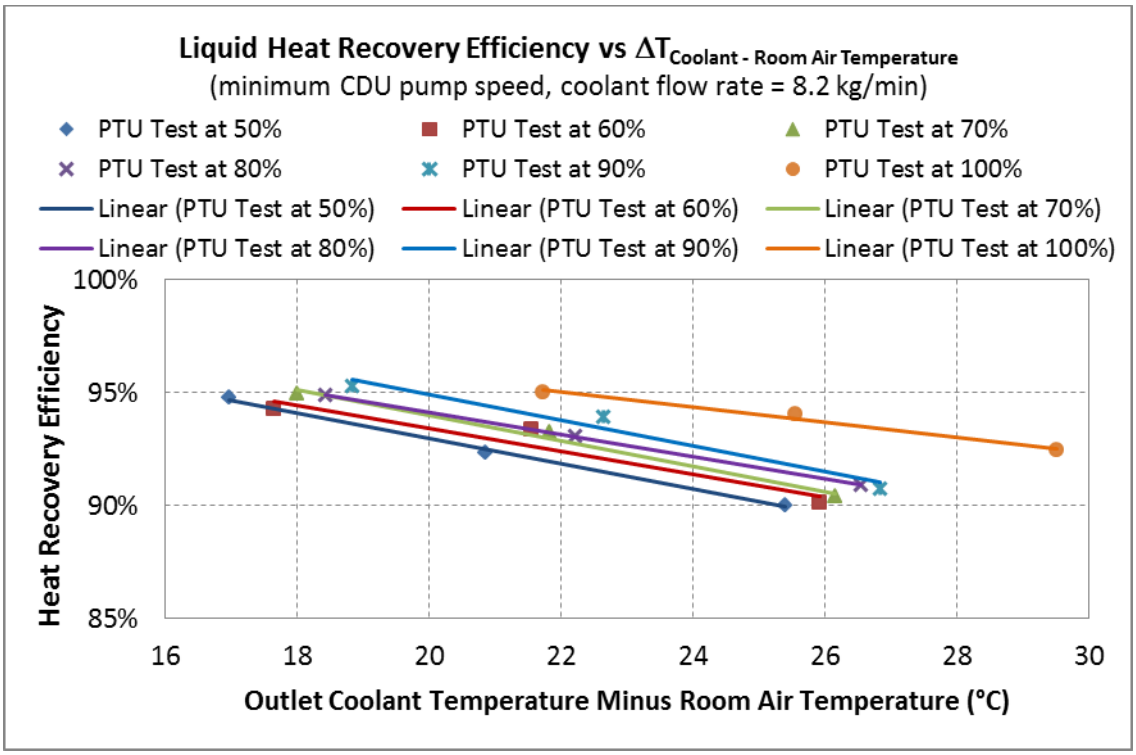

Figure 21. Heat recovery efficiency versus delta coolant/room air temperature (AVX tests not shown)

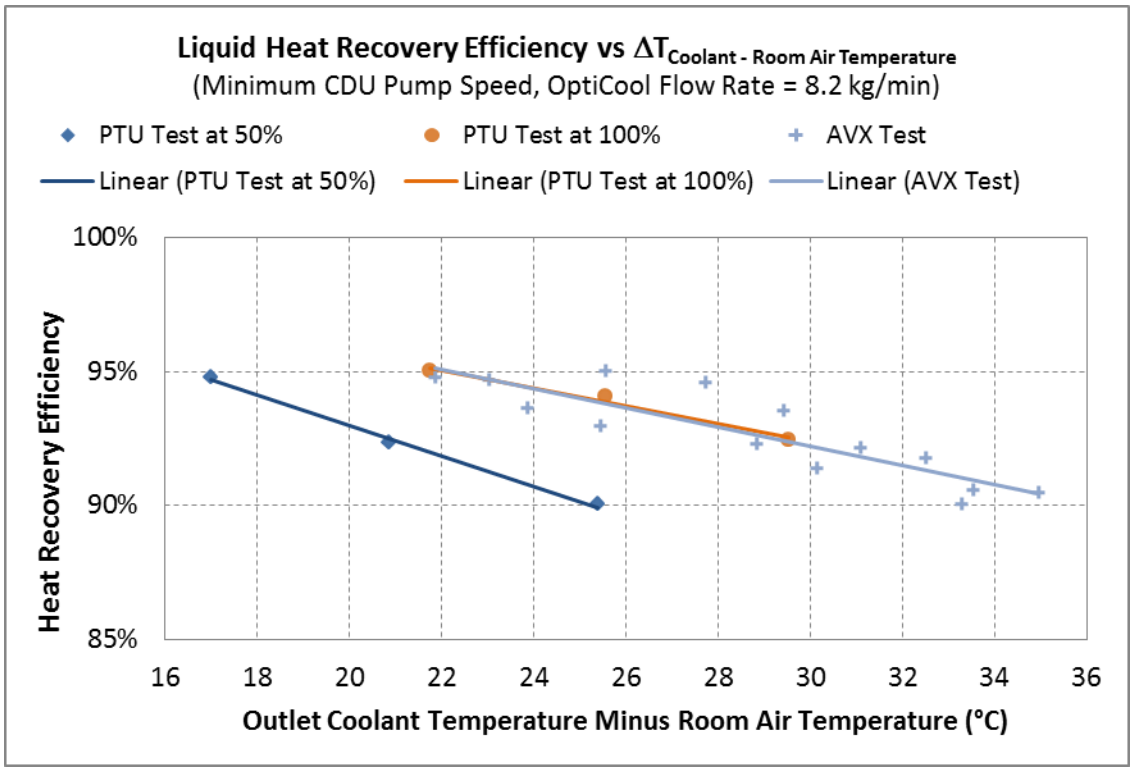

Figure 22. Heat recovery efficiency versus delta coolant/room air temperature (AVX tests shown)

Figure 23 shows the CDU power and coolant flow versus the CDU setting (which is software selectable). The CDU's coolant flowrate set point was an arbitrary input value (with an input range from 0 to 1,024) set to 500, 750, and 1,000, which correlated to 8.2, 12.7, and 14.5 kg/min. At 500, the CDU used about 23 W and sufficiently cooled the servers with computing power that ranged from 1,644 W to 3,131 W in our experiments. The CDU's control strategy increases pump speed up to a setting of 1,000 as necessary to maintain exiting coolant temperature less than 60°C, which occurs during instances of high water inlet temperature or reduced water flow. Maintaining the CDU speed at its minimum setting of 8.2 kg/min ensures the lowest possible power draw from the pump.

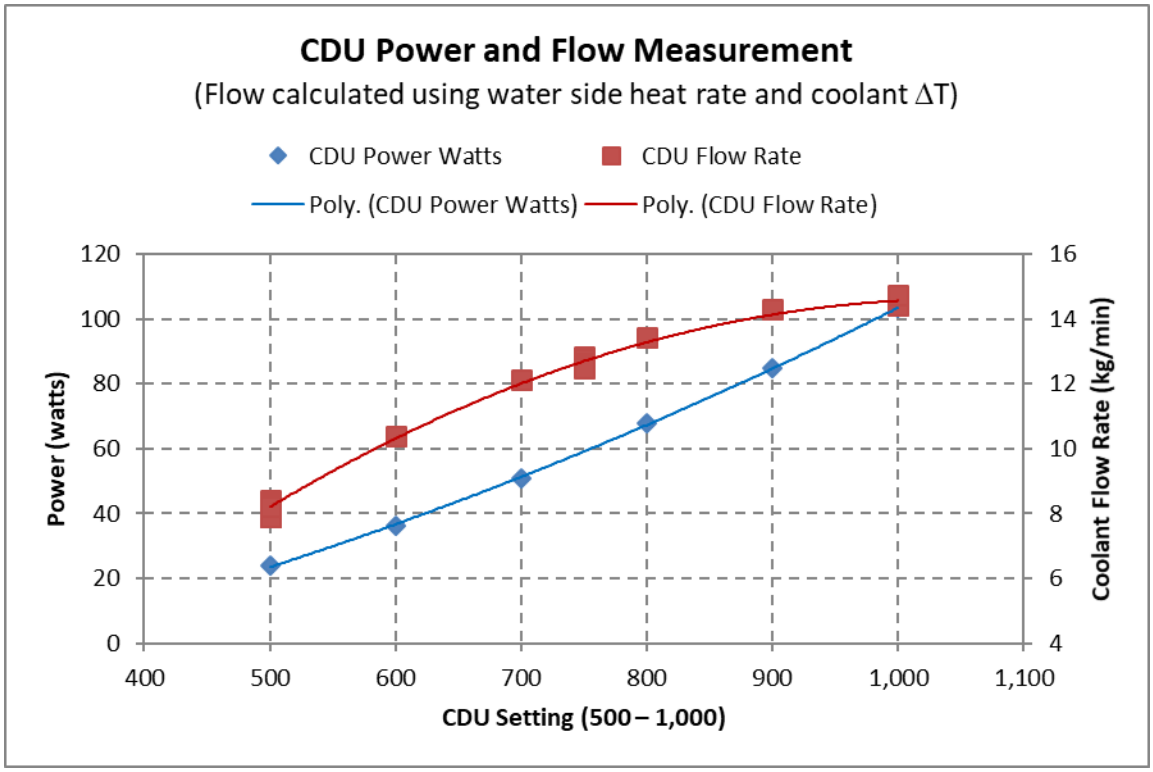

Figure 23. CPU power and flow measurement

When the CDU rejects heat to hot ambient conditions (e.g., with a water to air radiator) or to a building's hot water heating loop, the return water temperature to the CDU will be high (e.g. approaching 50°C). To reject the server heat, the water flow must then increase to maintain hot coolant temperature below 60°C. It is under these conditions that the CDU's heat exchanger's size must be determined. Figure 24 shows how well the heat exchanger in the experimental CDU performed. At low water-flow rates and high water-temperature rise, the effectiveness of the internal heat exchanger performed near the maximum of 100%. However, the effectiveness drops to about 43% when water is increased to 4.6 kg/min and dielectric coolant flow is 8.2 kg/min. Increasing the CDU's heat exchanger size to provide 80% or higher effectiveness is recommended at these higher flows, which coincide with the transition from water limited to coolant limited heat transfer. This will ensure effective heat rejection to ambient surroundings during warm ambient air conditions (e.g., summer days) and acceptable delivered water temperature during cold winter days.

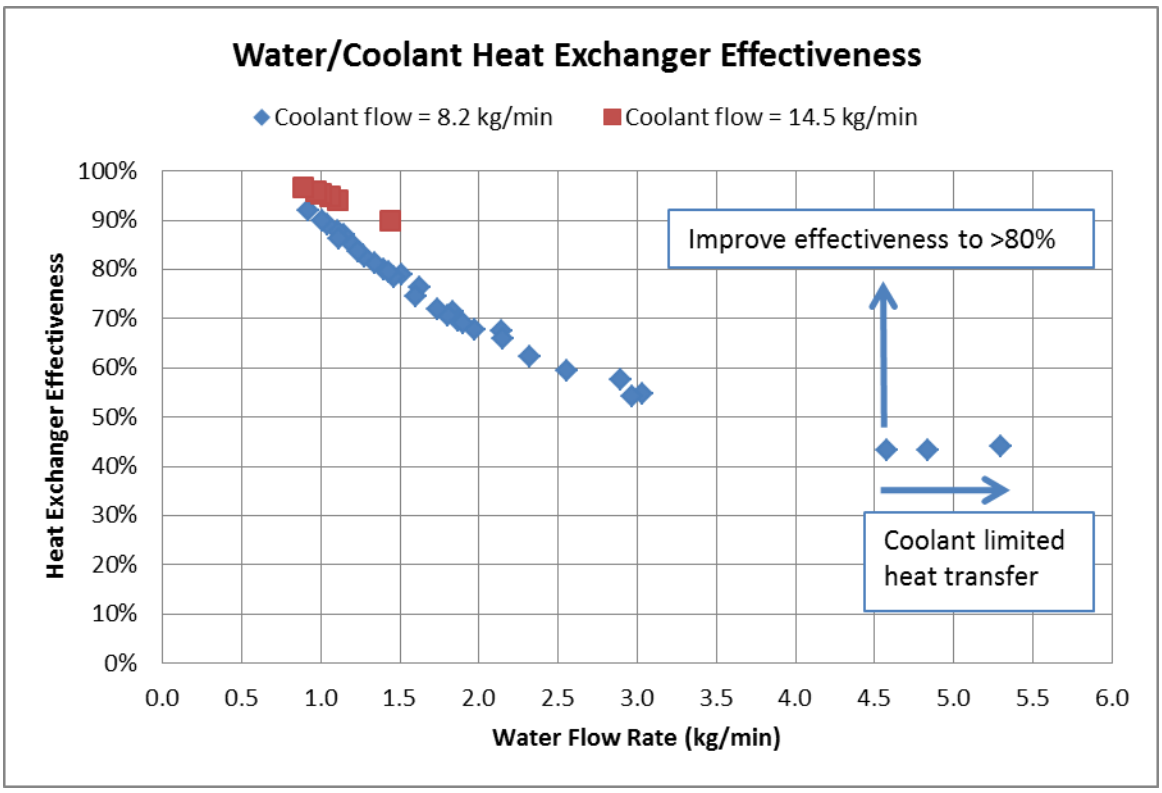

Figure 24. CPU coolant/water heat exchanger effectiveness

3 Phase Two: Pilot Demonstration at NREL's High-Performance Computing Data Center

3.1 Phase Two Objectives

The objectives of demonstrating the LSS technology at NREL's High-Performance Computing (HPC) Data Center[7] were to:

1. Determine system design suitable for acceptable performance in a liquid cooled data center
2. Determine operational characteristics in data center environment and verify acceptable thermal performance
3. Record and report observations of the LSS system.

3.2 Pilot Demonstration Description

Following the experiments performed at the Thermal Test Facility, the LSS system was installed at NREL's HPC Data Center in the ESIF. To understand the design requirements to run the LSS system, the ESIF's infrastructure must first be explained. Figure 25 shows a simplified process schematic of the ESIF's water cooling system used to reject server heat from the computing systems in the HPC. Shown, is the relevant connection process that delivers cooled water to the LSS rack and its CDUs. The supplied energy recovery water (ERW) to the servers is controlled to between 18.3°C and 23.9°C with the infrastructure expecting approximately 35°C or above return water temperature. Appendix F: HPC Data Center Cooling Overview Schematic shows a more detailed schematic of the ESIF's cooling system along with the other computing equipment serviced by the ERW cooling system.

During heating time of the year, approximately 0%–40% of the heat from the ERW is rejected to the ESIF's low temperature radiant heating system. The amount of heat reuse is currently limited by the necessity to provide ERW supply temperature (less than 24°C) that is below the required reuse temperature (typically in the range of 30°C to 40°C), which is dictated by the buildings radiant heating system. Therefore, once the heating system has reduced the ERW temperature to about 30°C, the rest of the heat in the ERW must be rejected to ambient. Furthermore, during cold winter days, the required reuse temperature often rises above 35°C, thus reducing the energy recovery from the data center to near 0%.

Knowing the stated thermal limitations of NREL's HPC data center, the LSS system was installed to reject heat at 50°C specifically to demonstrate its ability to improve heat recovery. Furthermore, the technology can be pushed to near 60°C heat rejection temperature with small improvements in the CDU's heat exchanger performance. However, this demonstration will not measurably improve NREL's HPC data center performance, as the LSS rack will add a mere 3 kW of computing to the near 1,000 kW of computing that currently exists.

The LSS system was modified from the experimental setup at the Thermal Test Facility to include the following features:

[7] https://www.nrel.gov/computational-science/facilities.html

1. Replacement of the Explorer™ rack with a 42U APC AR3350 server rack
2. One LCS-RT computer for monitoring and protecting the LSS servers
3. Redundant CDUs in a master/slave configuration whereby:
    A. The master CDU monitors pump operation and controls coolant return temperature to a maximum of 60°C.
        i. Normal operation has the pump running at the minimum speed setting of 500 (refer to Figure 23).
        ii. The pump speed is increased using the CDUs internal controller as necessary to maintain 60°C exiting coolant temperature.
    B. Upon a master CDU fault or power-down, the slave CDU takes control.
    C. The two CDUs are placed on different power phases to protect against single phase power outages.
4. One valve controller and one pressure independent characterized control valve that maintains a 49°C exit ERW temperature from the CDUs. The valve is set to a minimum open position to maintain a 35°C exit ERW temperature when the servers are at idle. Raising the exit ERW temperature to near 60°C was not possible for this demonstration because of the limited heat transfer rate of the CDU's heat exchangers (as described in the phase one experimental results)
5. One dielectric coolant reservoir with ambient pressure reference that sits 6U spaces above the CDUs
6. One catch pan with absorbent material below the rack to capture potential fluid spills or leaks
7. Local area network to provide computing resource for NREL's buildings research groups to develop OpenStudio Server (OS Server) and use this platform to perform building energy simulations for ongoing research.

The above system was reviewed by NREL's environmental, health, safety, and quality procedures and allowed to operate as designed with the following precautions:

1. Cabinet signs that read, "Caution: Hot Surfaces and Fluids! Temperatures up to 140°F are possible"
2. System cool down to less than 49°C prior to handling the servers
3. Absorbent pads and nitrile gloves available to staff for maintenance of the rack system
4. The servicing of the internal electronic components of the servers to be done with:
    A. Fill drain station provided by LCS with table top work surface area
    B. Absorbent pads available to set wet parts on
    C. Nitrile gloves and eye goggles for the service technician.

In practice, the surface and fluid temperatures did not pose any significant hindrance to the access of the computing systems. There were minor drips from the servers, but they have not

interfered with normal operation of all equipment in the rack, nor were they severe enough to reach the catch pan that was placed under the rack. Not every drip's source was identified; however, some appear to originate in a small printed circuit board that protrudes through the wet/dry interface at the front of the LSS enclosure. LCS will address the design of this interface in future hardware versions. For this demonstration, the servers were sent to LCS for servicing.

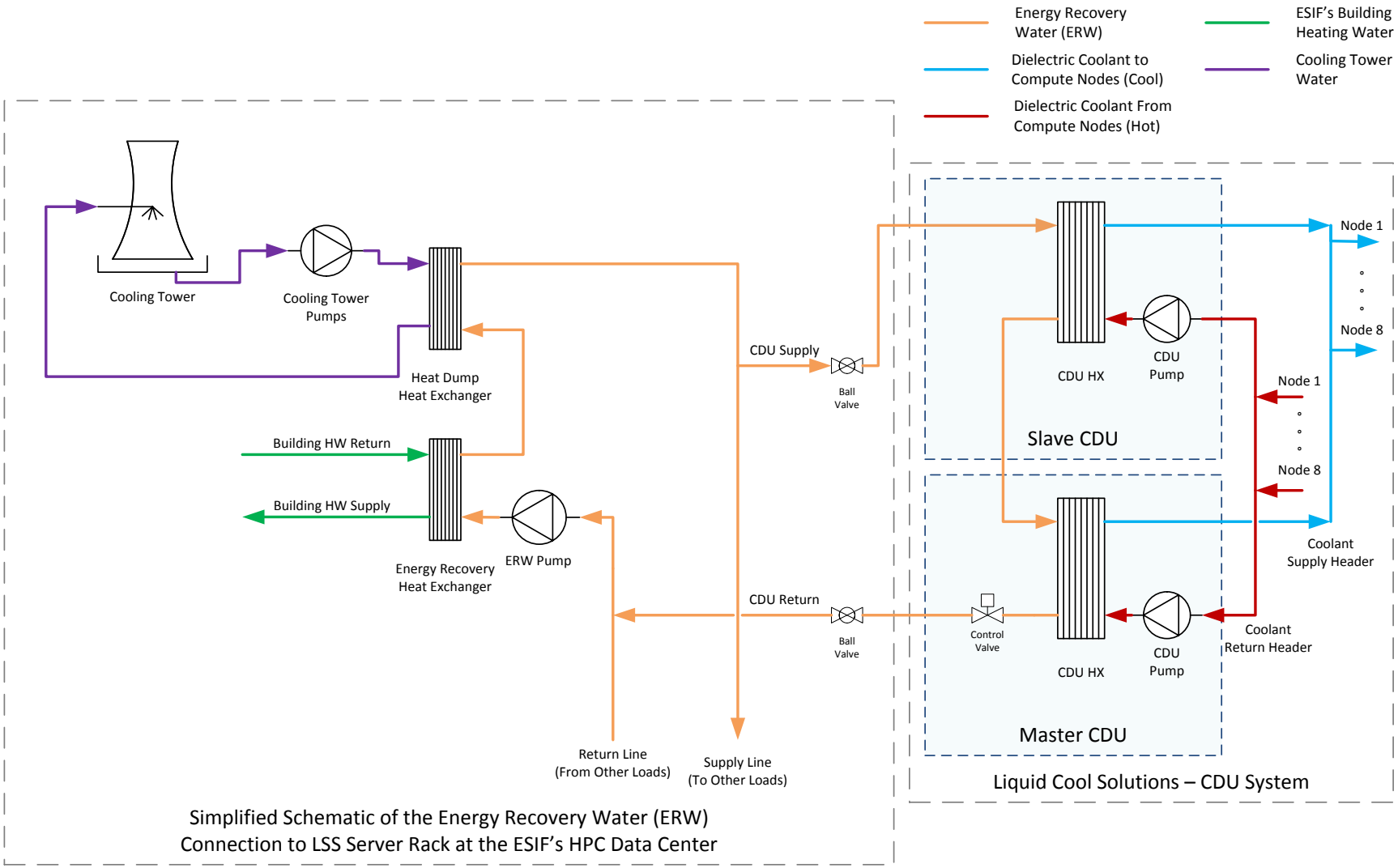

Figure 25. Process schematic showing fluid flows of the LSS server rack installed at NREL's HPC data center at the ESIF. A more detailed schematic can be found in Appendix F: HPC Data Center Cooling Overview Schematic. In this diagram, the LSS system is located at "Other Liquid Systems."

Figure 26 shows the back and front of the 42U server rack. In the back of the rack, the eight servers are connected via steel hoses to cool and hot fluid manifolds. The servers, hoses, manifolds, and CDUs were all equipped with drip-free quick connect fluid couplings, which allowed the installation to be completed quickly and easily. The headers are then connected to the two CDUs via parallel fluid connections. The control valve (orange) and controller (grey box with illuminated screen) sit above the servers. The ERW is delivered through the floor and through high pressure steel-reinforced fluid lines (hydraulic fluid lines). The front of the rack shows the location of the eight servers with the two CDUs above them. At the top is the monitoring system, which is liquid-cooled with self-contained radiators (shown in blue).

Since this was an early stage prototype, the hydraulic fluid hoses and connectors were chosen to minimize the chance of leaks due to pressure or connecting interfaces. These hoses can withstand pressures about 1,000 times or more than the fluids they contain. Typical practice at NREL's HPC is to pressure test all hoses to 1.5 times the design working pressure. The dielectric fluid design pressure is <20 kPa-G. Therefore, future designs will select simpler, more economical hoses and connectors.

3.3 Commissioning

The commissioning process was split up into three experiments to enable confidence in reliable system performance. These experiments were designed to stress the thermal control system both statically and dynamically. The objective was to show seamless operation during normal computing loads and proper system operation or shutdown to protect the servers against mechanical or electrical faults that affect the cooling system.

Simulation of step change to high computational load:

The system was setup to run the INTEL PTU tests at 100% from a cold start in order to test the system's ability to dynamically provide cooling to the servers. This step change in server load showed that all CPUs temperatures were maintained below 80°C and coolant temperatures exiting the servers below about 60°C. The ERW water overshoot temperature exiting the CDUs was maintained to less than 5°C and settled to 49°C after about 10 minutes. The RT monitoring system showed that all the system's temperature readings were within the limits during this exercise.

Simulation of master CDU shutdown:

The system was setup to run the Intel PTU tests at 100% with the ERW allowed to reach its maximum 49°C exiting temperature. The Master CDU was then shut off using its own power switch to simulate a fault.

The system proceeded to detect the fault and began startup the slave CDU. However, the time required to transition to the slave CDU was too long, as the RT monitoring system detected CPU over temperature and signaled all the servers to shut down. This outcome provided two critical pieces of information for LCS:

1. The current CDU strategy detects a master pump has shut down prior to starting the slave pump from the stopped state. A more robust method would operate two pumps

simultaneously, such that ramp up of the back-up pump can occur seamlessly when low flow is detected.

2. The RT monitoring system correctly identified unsafe operation and signaled the servers to shut down.

Although the slave CDU was unable to maintain system operation during a master CDU fault, the system was allowed to operate because (1) the monitoring system was able to safely shutdown the servers, and (2) the anticipated use during the demonstration isn't critically dependent on server up time.

Long-term simulation of high computational load:

The eight servers were run continuously with the Intel PTU software from Sept. 28 through Oct. 10, 2016, almost two weeks of continual operation. The purpose was to show that operation could withstand normal disturbances in the ESIF's ERW temperature and pressure fluctuations. The CPU temperatures were maintained below 77°C throughout the duration of the experiments with typical operation steady within ±2°C. All CPU temperatures were on average below 74°C. No computing anomalies were recorded.

Figure 26. Left: Eight-server rack from the back. Right: Eight server rack from the front
Photo by Dennis Schroeder, NREL

3.4 Operational Results Using Building Energy Simulation Software

NREL's commercial buildings program configured three servers to run the OS Server to support the software development of the platform and service the group's other simulation research needs. The OS Server platform is used to disseminate, to multiple server nodes, many single-instance building energy simulations using the OpenStudio® Software Development Kit.[8] In this stage of the project, three of the eight server nodes were used to run building energy simulations. Programing issues in the development version of OS Server software prevented operation of all eight servers. These issues were independent of the server hardware.

Data were recorded at approximately two-second intervals and captured CPU use and CPU temperature. Figure 27 and Figure 28 show the CPU use and CPU temperatures respectively for node 1 during a nine-hour computing period. This node showed the highest peak and range of CPU use, between 10% and 90%. The same data plotted using a two-minute running average (60 per. Mov. Avg.) show a maximum of 55% CPU use that gradually decreased to about 30%. The recorded CPU temperatures were maintained between about 50°C and 67°C. The experiment started with all eight servers at idle and CPU temperatures below 40°C and exiting ERW at about 35°C. As the compute power rose to steady levels, the ERW exiting temperature also rose to a steady 49°C.

Similarly, Figure 29 and Figure 30 show the CPU use and CPU temperatures respectively for node 4 for the same nine-hour computing period. Node 4 was measured to have the highest continuous computational load of the three servers. Figure 31 shows the two-minute running average of the CPU temperatures. CPU temperatures were held at or below 70°C. Maximum perturbation of CPU temperature was measured to be less than 6°C above the two-minute running average.

Figure 32 and Figure 33 show the CPU use and CPU temperatures respectively for node 8 for the same nine-hour computing period. The computational load for node 8 was between that of nodes 1 and 4. The CPU temperatures were held at or below 66°C.

The LSS system has successfully demonstrated its ability to maintain thermal control of eight servers at NREL's liquid cooled HPC data center. The system will continue to support NREL's buildings program[9], through September 2018, by providing a computing platform for researchers to simulate building energy-efficiency measures using the OS Server platform. Furthermore, the demonstration shows the viability of the technology to reject heat at 50°C, and with some minor design improvements, heat reject up to 60°C. Engineering changes to the CDU design and control are still needed to assure seamless coolant supply to the servers during a single pump failure.

[8] More information at https://www.openstudio.net/
[9] https://www.nrel.gov/buildings/

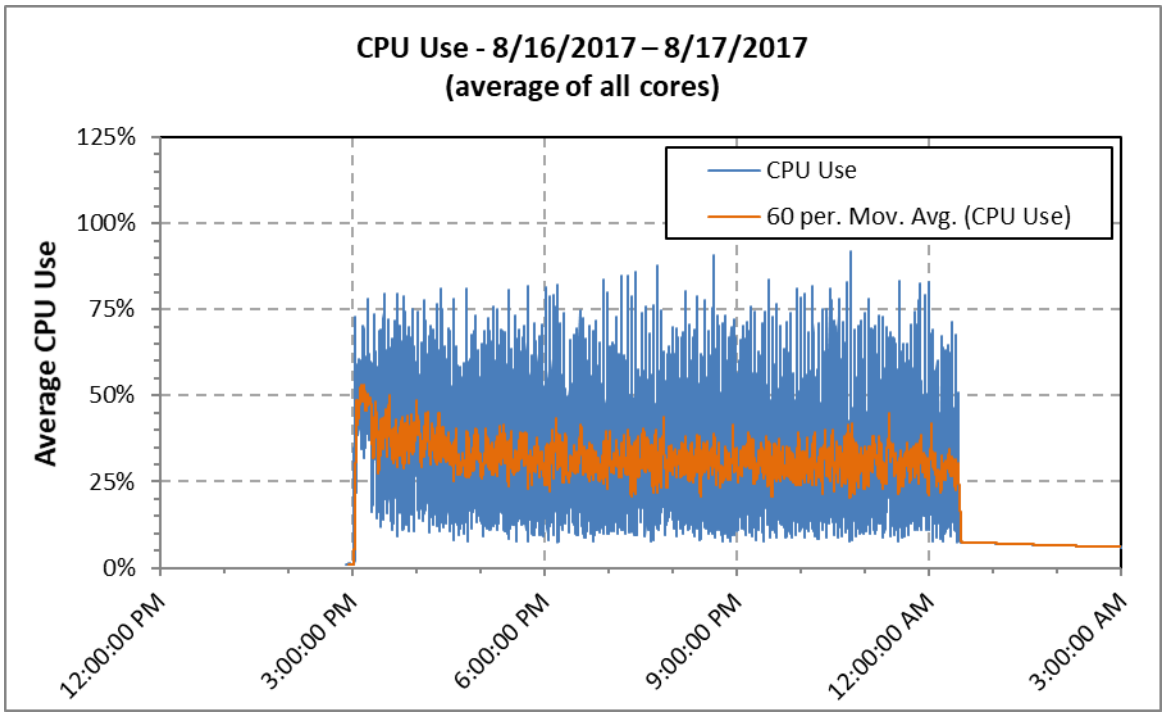

Figure 27. Node 1 average CPU use with a two-minute moving average (60 per. Mov. Avg.)

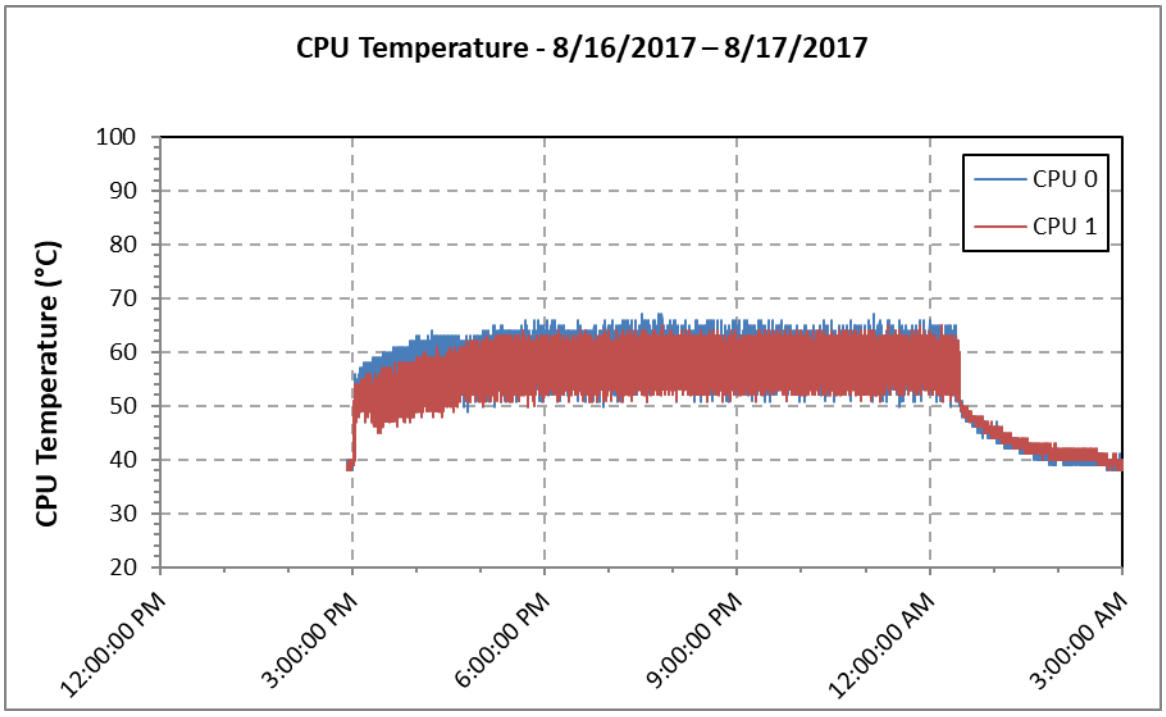

Figure 28. Node 1 CPU temperatures

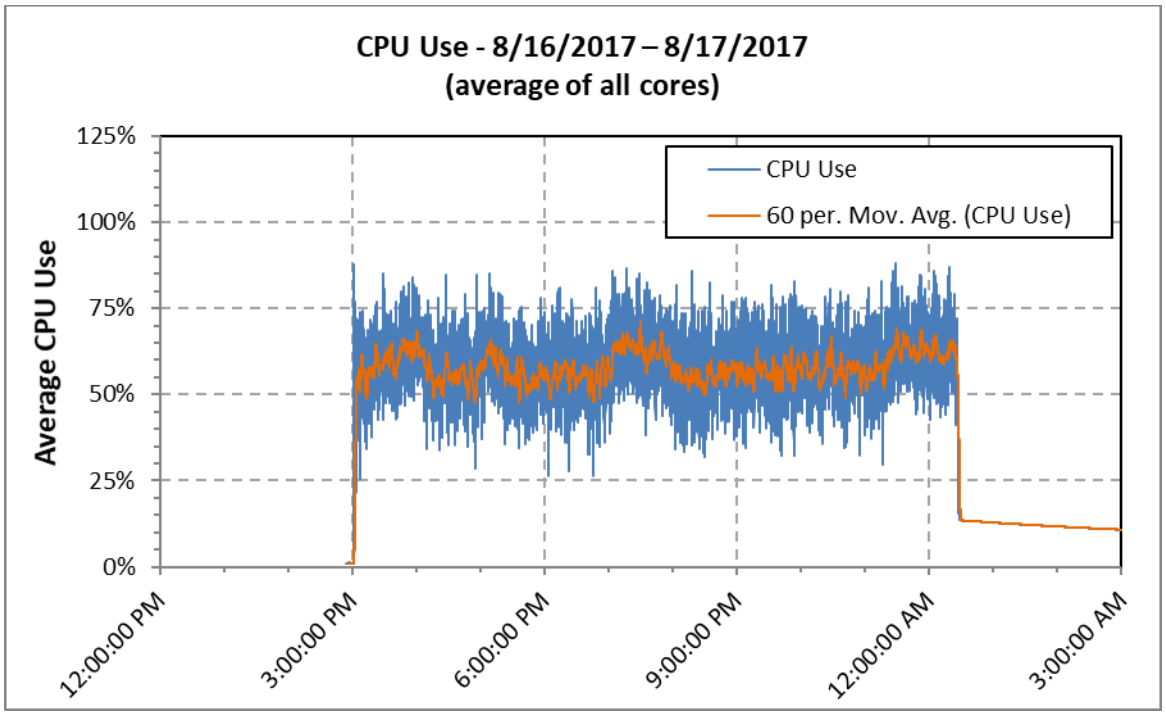

Figure 29. Node 4 average CPU use with a two-minute moving average (60 per. Mov. Avg.)

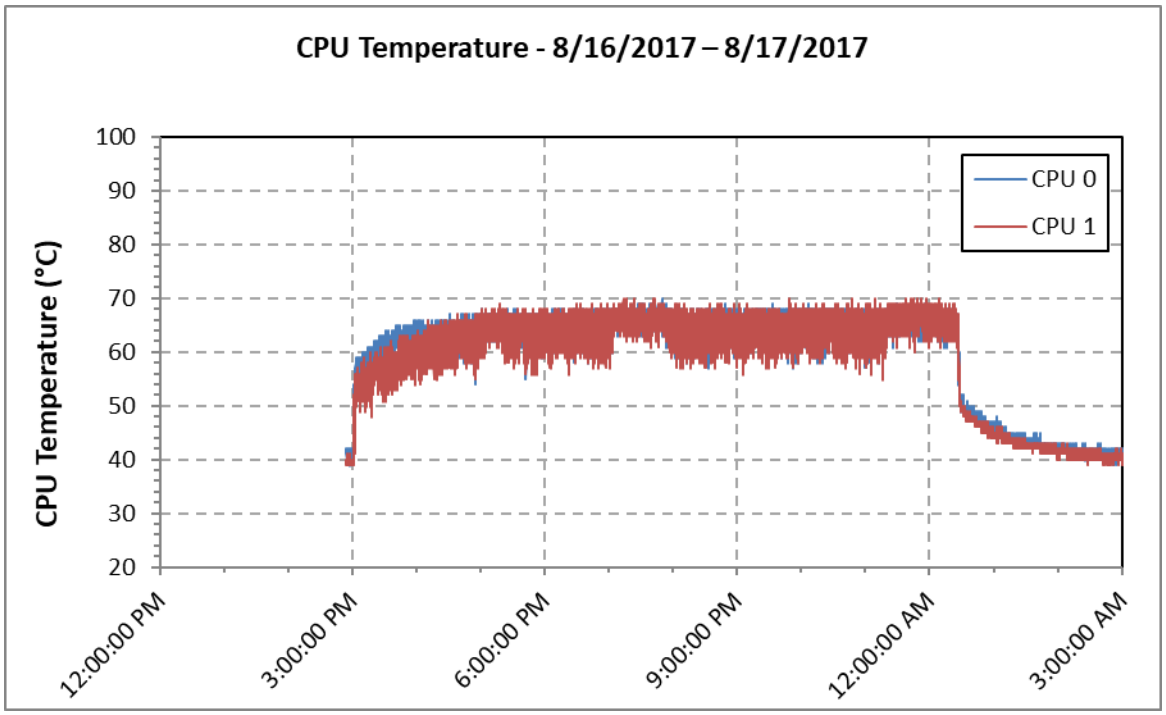

Figure 30. Node 4 CPU temperatures

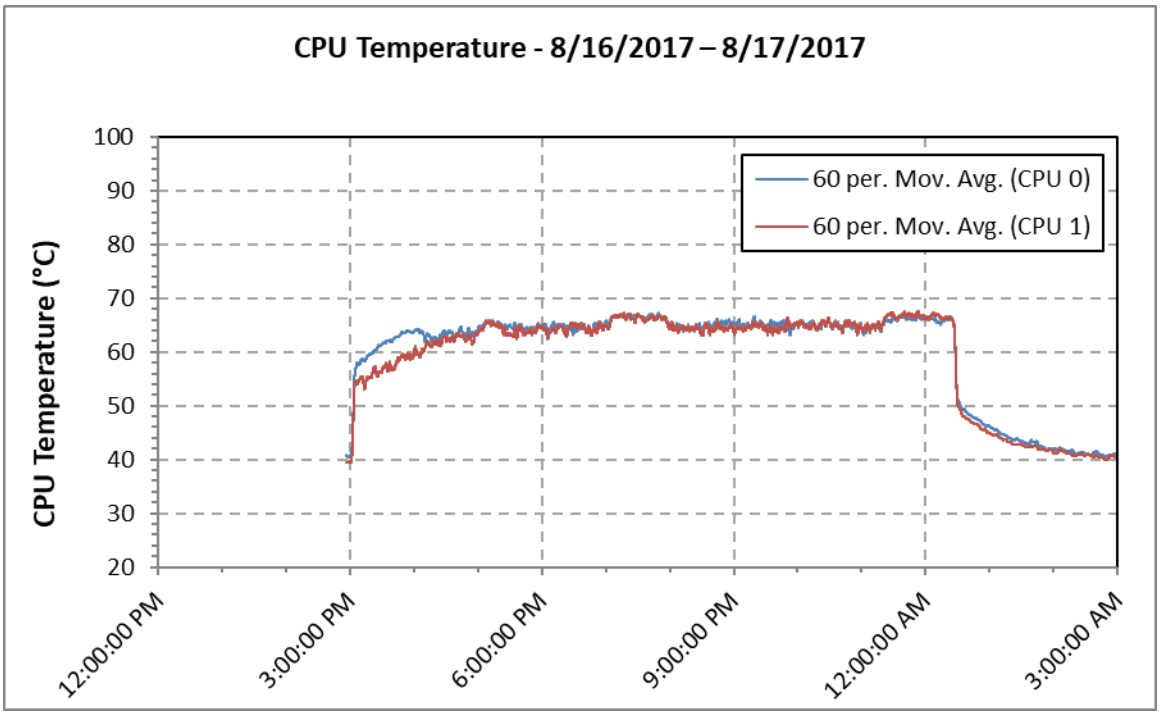

Figure 31. Node 4 CPU temperatures using a two-minute moving average (60 per. mov. avg.)

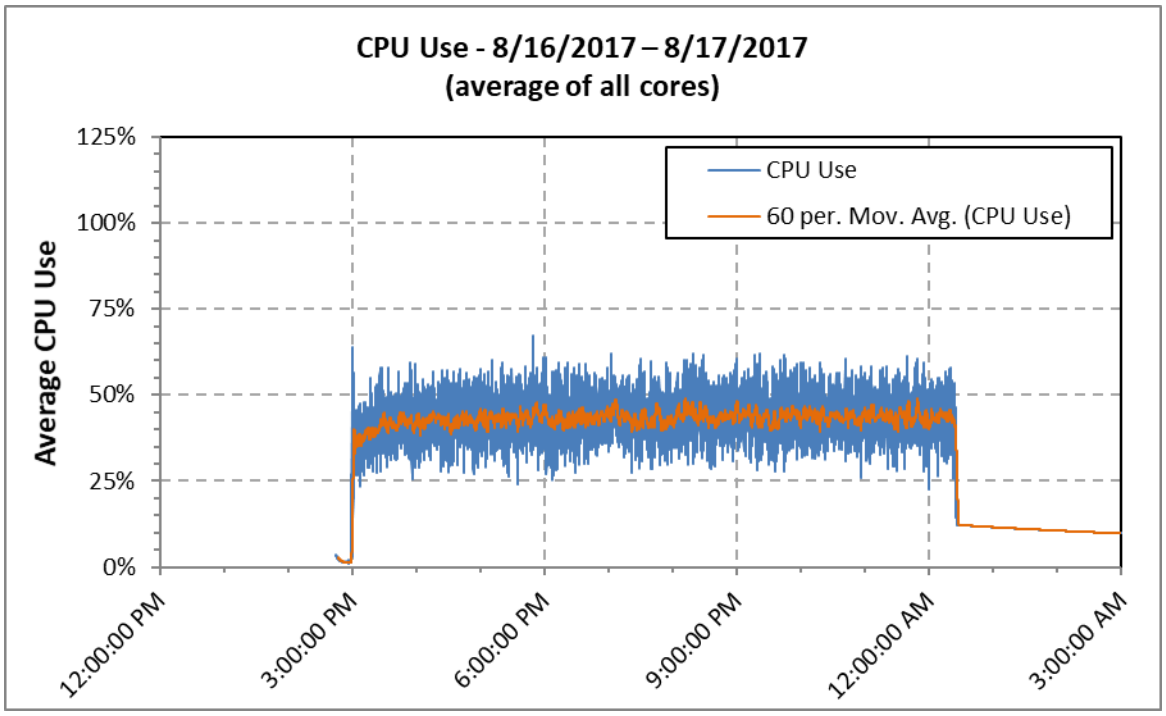

Figure 32. Node 8 average CPU use with a two-minute moving average (60 per. mov. avg.)

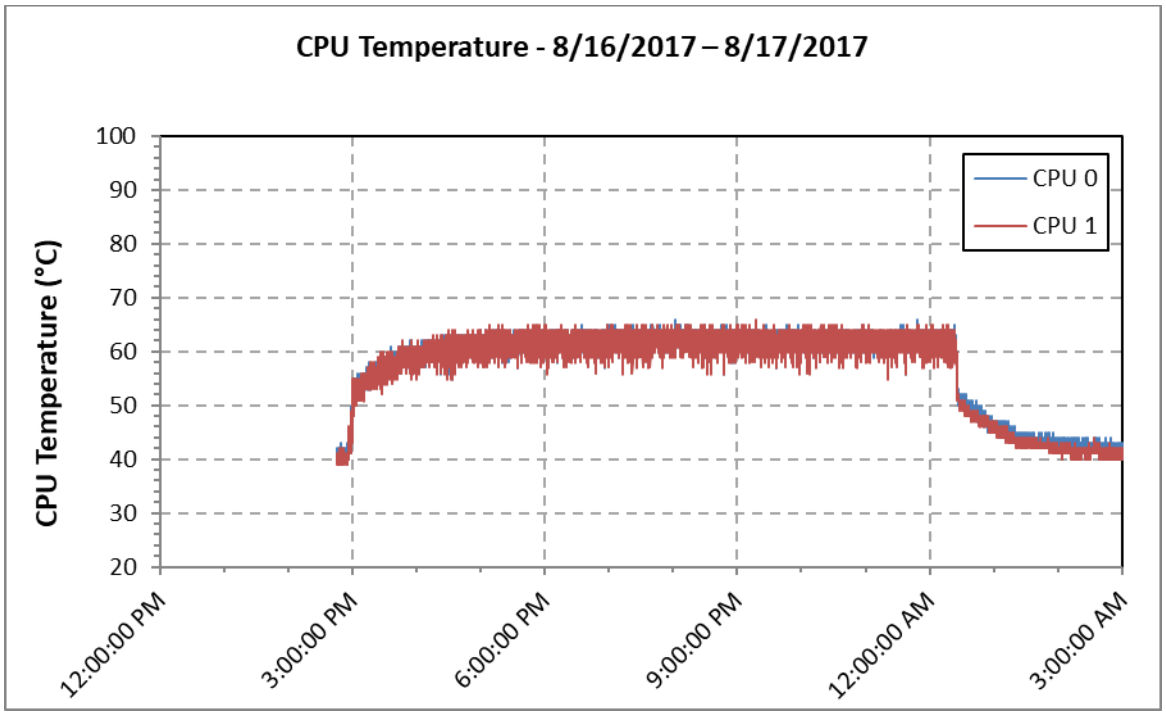

Figure 33. Node 8 CPU temperatures

Appendix A: Experiment Matrix

Table 1. Test Matrix

Test	Test Name	Date Complete	Water temp in	Water temp out	CDU Pump Speed	Air temp in	LSS Script	Air Flow Rate out of Calorimeter	Air Flow Rate into Calorimeter + Guard
		MM/DD/YYYY	°C	°C	%	°C	[description]	scmh	scmh
01	LiquidCool_Test01	10/20/2015	23.9	n/a	500	25.6	PTU - 100%	100	200
02	LiquidCool_Test02	10/20/2015	30.0	n/a	500	25.6	PTU - 100%	100	200
03	LiquidCool_Test03	10/20/2015	35	n/a	500	25.6	PTU - 100%	100	200
04	LiquidCool_Test04	10/21/2015	40	n/a	500	25.6	PTU - 100%	100	200
04-2	LiquidCool_Test04-2		40	n/a	500	25.6	PTU - 100%	100	200
05	LiquidCool_Test05	10/22/2015	25.6	48.9	500	25.6	Prime95 - 100%	100	200
06	LiquidCool_Test06	10/22/2015	25.6	48.9	500	25.6	PTU - 100%	100	200
07	LiquidCool_Test07	10/22/2015	25.6	48.9	500	25.6	PTU - 90%	100	200
08	LiquidCool_Test08	10/22/2015	25.6	48.9	500	25.6	PTU - 80%	100	200
09	LiquidCool_Test09	10/22/2015	25.6	48.9	500	25.6	PTU - 70%	100	200
10	LiquidCool_Test10	10/22/2015	25.6	48.9	500	25.6	PTU - 60%	100	200
11	LiquidCool_Test11	10/22/2015	25.6	48.9	500	25.6	PTU - 50%	100	200
12	LiquidCool_Test12	10/29/2015	23.9	48.9	500	25.6	PTU - max	100	200
13	LiquidCool_Test13	10/29/2015	30.0	48.9	500	25.6	PTU - max	100	200
14	LiquidCool_Test14	10/29/2015	35.0	48.9	500	25.6	PTU - max	100	200
15	LiquidCool_Test15	10/29/2015	40	48.9	500	25.6	PTU - max	100	200
16	LiquidCool_Test16	10/29/2015	15	48.9	500	25.6	PTU - max	100	200
17	LiquidCool_Test17	11/9/2015	15	43.3	500	25.6	PTU - max	100	200
18	LiquidCool_Test18	11/9/2015	23.9	43.3	500	25.6	PTU - max	100	200
19	LiquidCool_Test19	11/9/2015	30.0	43.3	500	25.6	PTU - max	100	200
20	LiquidCool_Test20	11/4/2015	35.0	43.3	500	25.6	PTU - max	100	200
21	LiquidCool_Test21	11/9/2015	23.9	43.3	500	25.6	PTU - 100%	100	200
22	LiquidCool_Test22	11/9/2015	23.9	43.3	500	25.6	PTU - 90%	100	200
23	LiquidCool_Test23	11/9/2015	23.9	43.3	500	25.6	PTU - 80%	100	200
24	LiquidCool_Test24	11/9/2015	23.9	43.3	500	25.6	PTU - 70%	100	200
25	LiquidCool_Test25	11/9/2015	23.9	43.3	500	25.6	PTU - 60%	100	200
26	LiquidCool_Test26	11/9/2015	23.9	43.3	500	25.6	PTU - 50%	100	200
27	LiquidCool_Test27	11/9/2015	15	37.8	500	25.6	PTU - max	100	200
28	LiquidCool_Test28	11/9/2015	20	37.8	500	25.6	PTU - max	100	200
29	LiquidCool_Test29	11/11/2015	23.9	37.8	500	25.6	PTU - max	100	200
30	LiquidCool_Test30	11/11/2015	30.0	37.8	500	25.6	PTU - max	100	200
31	LiquidCool_Test31	11/11/2015	23.9	37.8	500	25.6	PTU - 100%	100	200
32	LiquidCool_Test32	11/11/2015	23.9	37.8	500	25.6	PTU - 90%	100	200
33	LiquidCool_Test33	11/11/2015	23.9	37.8	500	25.6	PTU - 80%	100	200
34	LiquidCool_Test34	11/11/2015	23.9	37.8	500	25.6	PTU - 70%	100	200
35	LiquidCool_Test35	11/11/2015	23.9	37.8	500	25.6	PTU - 60%	100	200
36	LiquidCool_Test36	11/11/2015	23.9	37.8	500	25.6	PTU - 50%	100	200
37	LiquidCool_Test37	12/1/2015	~13.5	~23.5	500	25.6	PTU - max	100	200
38	LiquidCool_Test38	12/1/2015	23.9	51.7	500	25.6	PTU - max	100	200
39	LiquidCool_Test39	12/16/2015	23.9	48.9	750	25.6	PTU - max	100	200
40	LiquidCool_Test40	12/16/2015	23.9	48.9	750	25.6	PTU - 100%	100	200
41	LiquidCool_Test41	12/16/2015	23.9	48.9	750	25.6	PTU - 90%	100	200
42	LiquidCool_Test42	12/16/2015	23.9	48.9	750	25.6	PTU - 80%	100	200
43	LiquidCool_Test43	12/16/2015	23.9	48.9	750	25.6	PTU - 70%	100	200
44	LiquidCool_Test44	12/16/2015	23.9	48.9	750	25.6	PTU - 60%	100	200
45	LiquidCool_Test45	12/16/2015	23.9	48.9	750	25.6	PTU - 50%	100	200
46	LiquidCool_Test46	12/17/2015	23.9	48.9	1000	25.6	PTU - 100%	100	200
47	LiquidCool_Test47	12/17/2015	23.9	48.9	1000	25.6	PTU - 90%	100	200
48	LiquidCool_Test48	12/17/2015	23.9	48.9	1000	25.6	PTU - 80%	100	200
49	LiquidCool_Test49	12/17/2015	23.9	48.9	1000	25.6	PTU - 70%	100	200
50	LiquidCool_Test50	12/17/2015	23.9	48.9	1000	25.6	PTU - 60%	100	200
51	LiquidCool_Test51	12/17/2015	23.9	48.9	1000	25.6	PTU - 50%	100	200
53	LiquidCool_Test53	12/17/2015	23.9	48.9	600	25.6	PTU - max	100	200
54	LiquidCool_Test54	12/17/2015	23.9	48.9	700	25.6	PTU - max	100	200
55	LiquidCool_Test55	12/17/2015	23.9	48.9	800	25.6	PTU - max	100	200
56	LiquidCool_Test56	12/17/2015	23.9	48.9	900	25.6	PTU - max	100	200
57	LiquidCool_Test57	12/17/2015	23.9	48.9	1000	25.6	PTU - max	100	200

Appendix B: Example of Detailed Output and Calculations

NREL
NATIONAL RENEWABLE ENERGY LABORATORY

Test Summary Spreadsheet for LiquidCool Solutions

Tests Performed By: Eric Kozubal, Lucas Philips

Testing performed at NREL's Advanced HVAC Systems Laboratory in Golden, CO

Test Name	Core Data File	Script	Test Date	Test Start	Test Finish	Duration
LiquidCool_Test01	CoreData_Test01.xlsb	PTU - 100%	10/20/2015	1:59:13 PM	2:29:13 PM	0:30:00

Color Key = Measurement | Calculation | Key metric | Set Point | Good / Pass | Bad / Fail

Server Measured States:

Rack Power

	Value	Units	Notes
Total Rack Power	2666	Watts	*Total power into PDU*
CDU Speed Setting	500	-	*setting value into CDU controller (range = 500-1024)*
CDU Power	23	Watts	*This value is calculated based on correllation of pump power from separate measurements*
PDU + Switch Power	9	Watts	*This value is based on separate measurement*
Power into servers	2634	Watts	*Electrical power into all 8 servers*

Processors - CPU0

	Head Node	Node 1	Node 2	Node 3	Node 4	Node 5	Node 6	Node 7	Units
Speed	2621	2616	2619	2618	2621	2616	2616	2618	MHz
Usage	100	100	100	100	100	100	100	100	%
Temperature	63.2	63.9	64.6	65.8	65.2	66.3	64.9	66.9	°C
Voltage	0.79	0.82	0.80	0.82	0.79	0.85	0.84	0.81	Volts
Power	99	102	100	104	102	106	104	105	Watts
Max. of Core Temperatures	62.1	63.2	64.2	65.6	65.1	65.6	63.6	63.9	°C
Min. of Core Temperatures	58.5	59.6	60.7	61.5	59.6	59.6	60.2	59.9	°C
Average of Core Temperatures	60.2	61.4	62.3	63.5	62.2	63.0	62.0	62.1	°C

Processors - CPU1

	Head Node	Node 1	Node 2	Node 3	Node 4	Node 5	Node 6	Node 7	Units
Speed	2613	2615	2617	2614	2618	2613	2612	2616	MHz
Usage	100	100	100	100	100	100	100	100	%
Temperature	65.4	62.6	63.6	65.8	65.0	66.8	66.3	65.7	°C
Voltage	0.82	0.83	0.82	0.83	0.84	0.82	0.85	0.82	Volts
Power	101	101	96	105	105	104	105	104	Watts
Max. of Core Temperatures	63.6	62.5	63.5	65.5	64.9	66.3	65.5	64.7	°C
Min. of Core Temperatures	59.3	58.7	57.2	60.5	59.5	61.5	60.9	60.8	°C
Average of Core Temperatures	61.5	60.5	60.8	62.8	61.7	63.7	63.0	62.8	°C

Memory - BANK0

	Head Node	Node 1	Node 2	Node 3	Node 4	Node 5	Node 6	Node 7	Units
Power	15.78	16.20	15.86	16.50	16.02	16.91	16.36	16.50	Watts
Max. Temperature (of 4 DIMMs)	60.0	61.0	61.0	60.6	61.0	61.1	61.0	60.0	°C

Memory - BANK1

	Head Node	Node 1	Node 2	Node 3	Node 4	Node 5	Node 6	Node 7	Units
Power	16.10	15.98	16.60	15.60	16.30	16.30	16.41	15.36	Watts
Max. Temperature (of 4 DIMMs)	60.0	59.8	59.2	59.0	60.0	61.0	60.0	59.0	°C

Air States

	Chamber In	Chamber Out	Units	Notes
Temperature	25.6	29.0	°C	*Air flow through the chamber was controlled such that this temperature rise ≤ 5°C*
Temperature Setpoint	25.6		°C	
Dew Point	12.0	12.0	°C	*This parameter was loosely controlled to between 8 and 12°C*
Ambient Air Pressure	82.3		kPa	
Relative Humidity	43%	35%		
Humidity Ratio	10.8	10.8	g/kg	
Density	0.944	0.933	kg/m^3	*Dry air density (kg of dry air per cubic meter)*
AirFlow	100	100	SCMH	*Standard air* $\rho = 1.2\ kg/m^3$
AirFlow Setpoint		100	SCMH	
AirFlow	127	129	CMH	
AirFlow	120	120	kg/hr	
Enthalpy	53.2	56.8	kJ/kg	
Thermal Power	119		Watts	*Heat removal by convection of air*

Fluid States (External to LSS)

	Cold Water	Hot Water	Cold Dielectric	Hot Dielectric	Units	Notes
Temperature	24.0	47.9	45.9	53.7	°C	
Temperature Setpoint	23.9	-9999.0	-	-	°C	*-9999 value indicates no setpoint used (e.g. thermal valve us*
Density	0.997	0.989	0.777	0.772	kg/l	*Dielectric fluid properties data provided by LCS*
Specific Heat	4.14	4.14	2.23	2.26	kJ/kg-C	*Dielectric fluid properties data provided by LCS*
Flow Rate	1.47	1.48	10.68	10.76	lpm	*Dielectric fluid flow inferred from heat rate*
Flow Rate	1.46		8.30		kg/min	*Dielectric fluid flow inferred from heat rate*
CDU Heat Rate	2413				Watts	*Water side heat rate of CDU heat exchanger*
CDU water-side HX effectiveness	80%					*"n/a" if Cmin is the dielectric fluid side*
Heat recovery percentage	92%				-	*Heat rate removed by CDU divided by power into servers*

Calorimeter Calculations

	Chamber In	Units	Notes
Power input	2666	Watts	*Electric input*
Heat output	2532	Watts	*Heat out by air and water*
Missing Power	134	Watts	*Un-accounted for power (Measurement and Systematic Error)*
Measurement Uncertainty	51	Watts	*Measuremnt error only*
Measurement Uncertainty	1.9%	-	*Measuremnt error only*
Energy Balance	1.053	-	*Power input divided by heat output*

Processor Calculations

Processors - CPU0

	Head Node	Node 1	Node 2	Node 3	Node 4	Node 5	Node 6	Node 7	Units
ΔT Core - fluid Inlet	17.2	18.0	18.7	19.9	19.2	20.4	18.9	21.0	°C
ΔT Average core - fluid Inlet	14.3	15.4	16.4	17.6	16.3	17.1	16.1	16.1	°C
Watts/°C using core temp	5.74	5.64	5.36	5.23	5.29	5.18	5.49	4.99	Watts/°C
Watts/°C using average core temp	6.92	6.58	6.12	5.91	6.26	6.17	6.47	6.48	Watts/°C
ΔT Dielectric fluid through CPU	5.1	5.3	5.2	5.4	5.3	5.5	5.4	5.4	°C
Dielectric fluid exiting temperature	51.1	51.2	51.1	51.3	51.2	51.4	51.3	51.4	°C
Percent of total temperature rise	66%	68%	67%	69%	68%	71%	69%	70%	

Processors - CPU1

	Head Node	Node 1	Node 2	Node 3	Node 4	Node 5	Node 6	Node 7	Units
ΔT Core - fluid inlet	19.5	16.7	17.7	19.9	19.1	20.9	20.4	19.8	°C
ΔT Average core - fluid inlet	15.6	14.5	14.9	16.9	15.8	17.8	17.0	16.8	°C
Watts/°C using core temp	5.08	6.09	5.65	5.22	5.34	5.06	5.10	5.29	Watts/°C
Watts/°C using average core temp	6.33	6.99	6.73	6.14	6.45	5.95	6.10	6.22	Watts/°C
ΔT Dielectric fluid through CPU	5.2	5.2	5.0	5.4	5.4	5.4	5.5	5.4	°C
Dielectric fluid exiting temperature	51.2	51.1	50.9	51.4	51.4	51.3	51.4	51.3	°C
Percent of total temperature rise	67%	67%	64%	70%	70%	69%	70%	70%	

Aggregated Performance

	Average	Minimum	Maximum	Standard Dev	Units	Notes
ΔT Core - fluid inlet	19.2	16.7	21.0	1.27	°C	
ΔT Average core - fluid inlet	16.2	14.3	17.8	1.04	°C	
Watts/°C using CPU temp	5.4	5.0	6.1	0.30	Watts/°C	*uses PTU reported CPU temperature*
Watts/°C using average core temp	6.4	5.9	7.0	0.32	Watts/°C	*uses average of all core temperatures per CPU (24 cores/CPU*
ΔT Dielectric fluid through CPU	5.3	5.0	5.5	0.14	°C	*Back calculation: Assumes equal flow through each CPU*
Dielectric fluid exiting temperature	51.3	50.9	51.4	0.14	°C	*Back calculation: Assumes equal flow through each CPU*
Percent of total temperature rise	68%	64%	71%	1.8%		
CPU Speed	2617	2612	2621	3	MHz	
CPU Usage	100	100	100	0.0	%	
CPU Temperature	65.1	62.6	66.9	1.27	°C	
CPU Voltage	0.82	0.79	0.85	0.018	Volts	
CPU Power	102.5	96.0	105.7	2.74	Watts	
Total CPU Power	1640				Watts	*All 16 CPUs*
Percent of total server power	62%					*Total CPU power ÷ Total server input power*

Memory Calculations

Memory - BANK0

	Head Node	Node 1	Node 2	Node 3	Node 4	Node 5	Node 6	Node 7	Units
ΔT Core - fluid outlet	6.3	7.3	7.3	6.8	7.3	7.3	7.3	6.3	°C
ΔT Core - fluid exiting CPUs	8.9	9.8	10.0	9.2	9.7	9.7	9.6	8.6	°C
Watts/°C using fluid exiting CPU	1.77	1.65	1.59	1.79	1.65	1.74	1.70	1.91	Watts/°C

Memory - BANK1

	Head Node	Node 1	Node 2	Node 3	Node 4	Node 5	Node 6	Node 7	Units
ΔT Core - fluid outlet	6.3	6.1	5.4	5.3	6.3	7.3	6.3	5.3	°C
ΔT Core - fluid exiting CPUs	8.9	8.6	8.1	7.7	8.7	9.6	8.6	7.6	°C
Watts/°C using fluid exiting CPU	1.81	1.86	2.04	2.04	1.87	1.69	1.90	2.01	Watts/°C

Aggregated Performance

	Average	Minimum	Maximum	Standard Dev	Units	Notes
Temperatures	60.2	59.0	61.1	0.75	°C	
ΔT Core - fluid outlet	6.5	5.3	7.3	0.75	°C	
ΔT Core - fluid exiting CPUs	9.0	7.6	10.0	0.75	°C	*Dielectric fluid exiting CPUs then cool the rest of the motherl*
Power	16.2	15.4	16.9	0.40	Watts	
Watts/°C using fluid exiting CPU	1.8	1.6	2.0	0.1	Watts/°C	
Total Memory Power	258.8				Watts	*All 16 DIMMs*
Percent of total server power	10%					*Total memory power ÷ Total server input power*

Figure 34. Example of detailed output and calculations

Appendix C: Reported Values for Each CPU or DIMM

Table 2. PTU Software Reported Values for Each CPU or DIMM

Variable	Unit	Added Description
CPU Frequency	MHz	Processor speed
CPU Usage	%	Processor usage
DTS		
Physical Temperature	°C	CPU core temperature
CPU Voltage	Volts	
CPU Power	watts	
T_Margin	°C	
Memory Temperature	°C	
Memory Power	watts	

Appendix D: Material Properties Used for Thermodynamic Calculations

Table 3. Dielectric Coolant (DSI Ventures Inc. – OptiCool™ 87252) Material Properties Used for Thermodynamic Calculations (Data provided by LCS)

Temp	Kinematic Viscosity	Dynamic Viscosity	Specific Heat	Thermal Conductivity	Specific Gravity	Density	Coefficient of Thermal Expansion	Volumetric Heat Capacity
°C	cSt	Poise	kJ/kg-K	W/m-K		kg/m3	(volume/K)	J/mL-K
0	18.8	0.1519	2.054	0.1381	0.8081	808.1	0.000673	1.660
10	12.5	0.1002	2.092	0.1381	0.8014	801.4	0.000673	1.676
20	8.82	0.0701	2.129	0.1381	0.7946	794.6	0.000673	1.692
30	6.52	0.0514	2.167	0.1381	0.7879	787.9	0.000673	1.707
40	5.00	0.0391	2.204	0.1358	0.7812	781.2	0.000673	1.722
50	3.96	0.0307	2.242	0.1358	0.7744	774.4	0.000673	1.736
60	3.22	0.0247	2.280	0.1358	0.7677	767.7	0.000673	1.750
70	2.69	0.0205	2.317	0.1358	0.7610	761.0	0.000673	1.763
80	2.27	0.0171	2.355	0.1358	0.7543	754.3	0.000673	1.776
90	1.95	0.0146	2.392	0.1358	0.7475	747.5	0.000673	1.788
100	1.70	0.0126	2.430	0.1323	0.7408	740.8	0.000673	1.800

Appendix E: Serial Number to Node Map

	Left Side							Right Side
Node -->	7	6	5	4	3	2	1	HN
SN -->	M2501008	M2501007	M2501006	M2501001	M2501002	M2501003	M2501009	M2501005

Figure 35. Serial number to node map (as viewed from the front)

Appendix F: HPC Data Center Cooling Overview Schematic

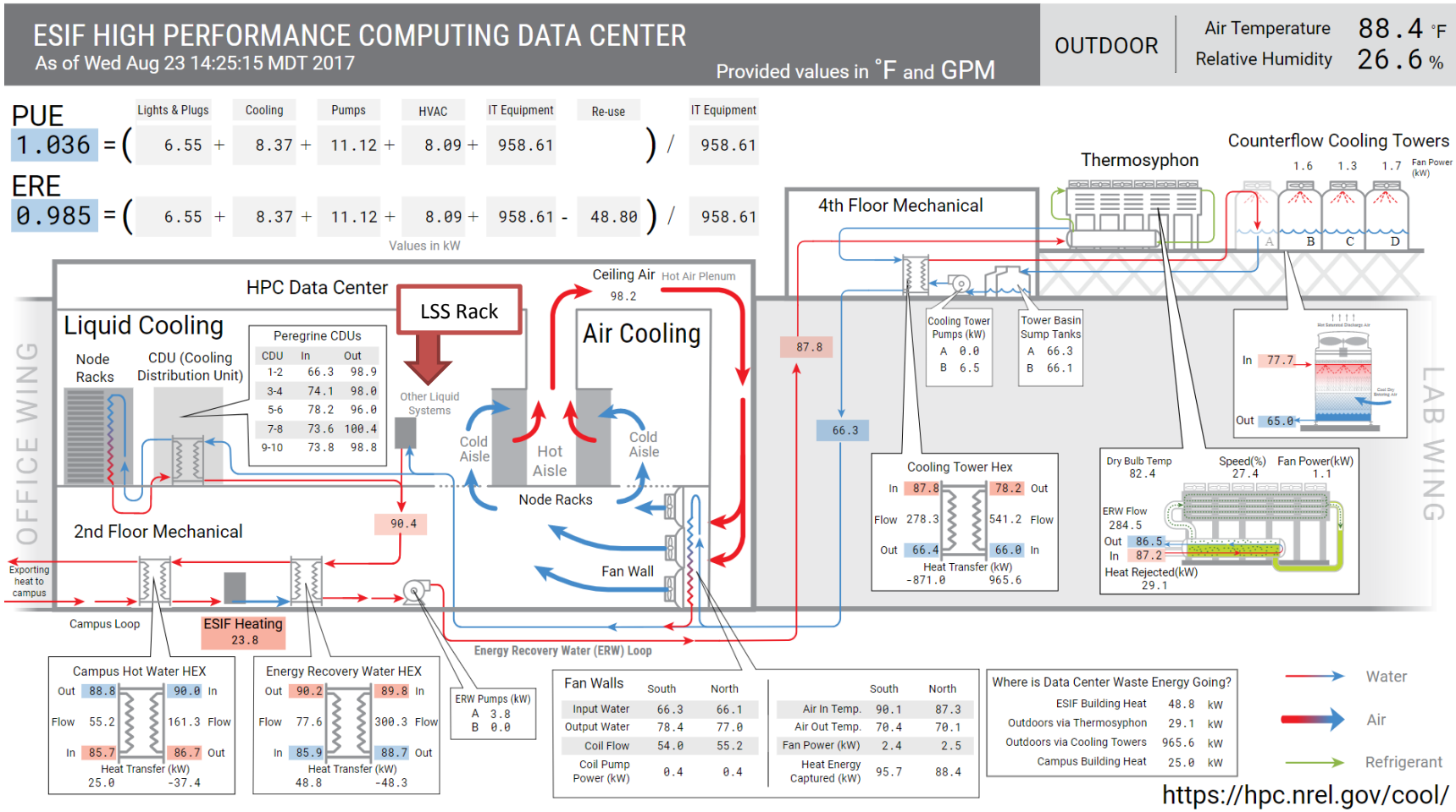

Figure 36. Screen capture of NREL's HPC data center cooling overview website (Aug. 23, 2017 at 2:25 p.m. MDT): https://hpc.nrel.gov/COOL/index.html

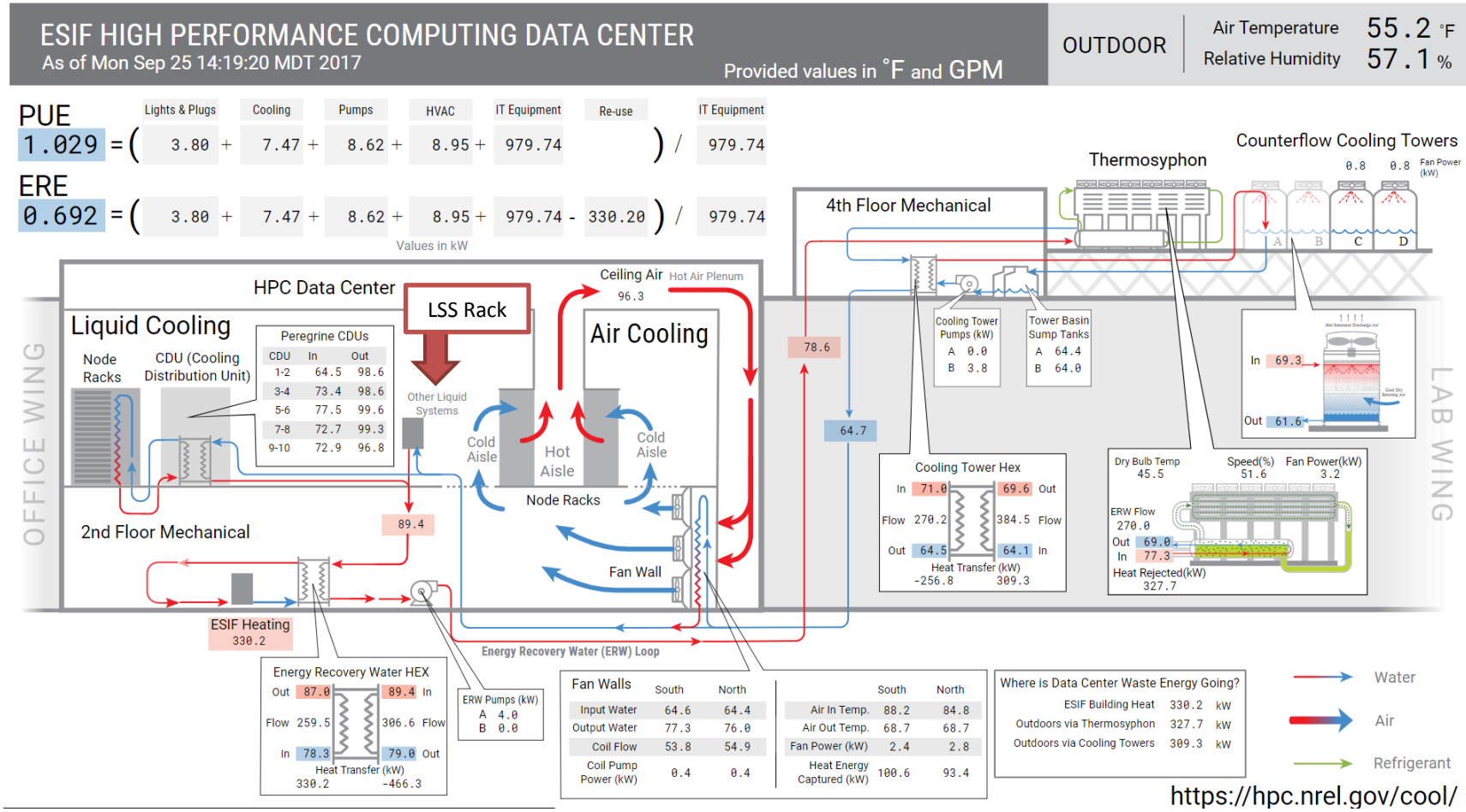

Figure 37. Screen capture of NREL's HPC data center cooling overview website (Sept. 25, 2017 at 2:19 p.m. MDT). Data shown in IP units: https://hpc.nrel.gov/COOL/index.html

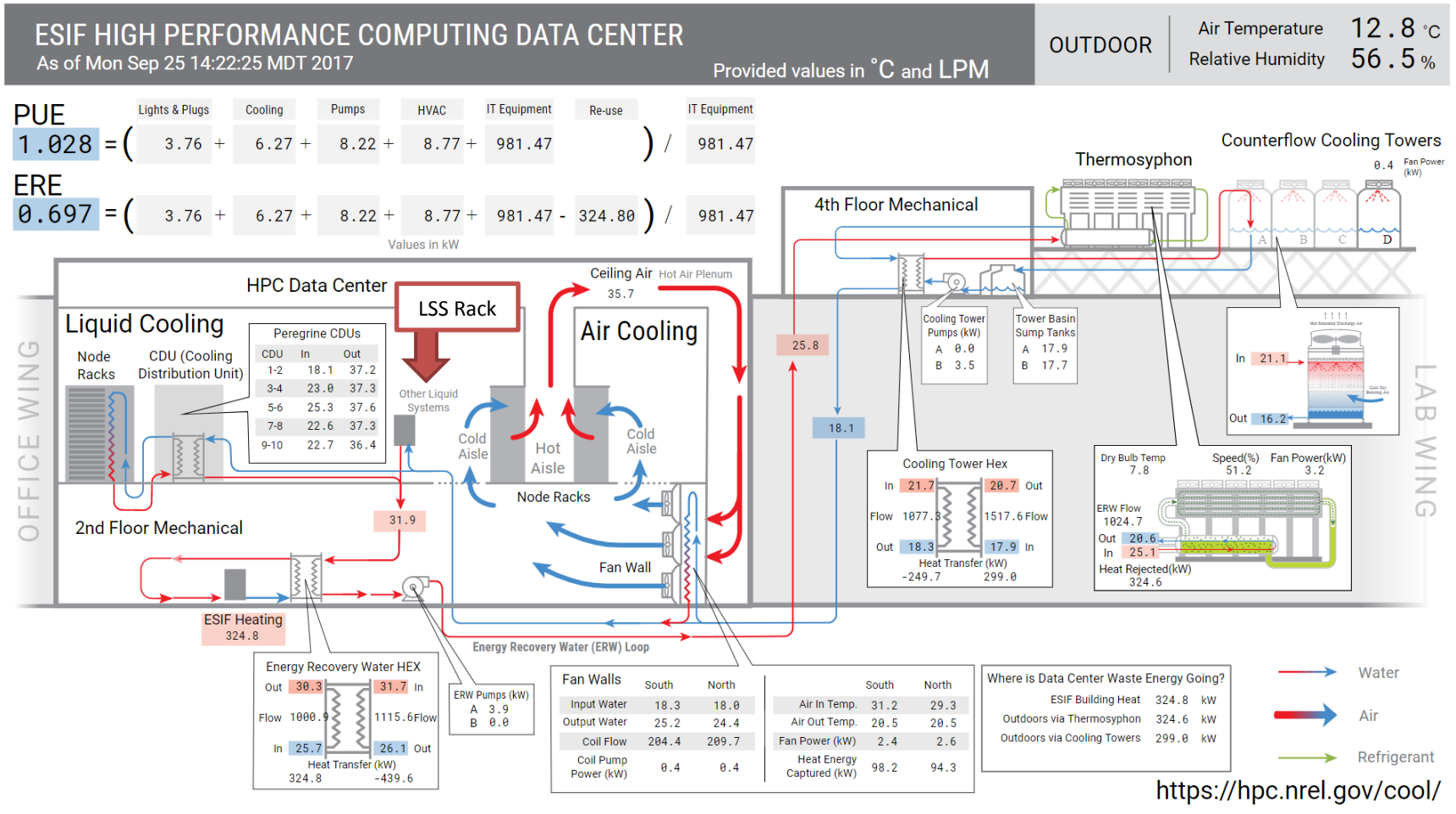

Figure 38. Screen capture of NREL's HPC data center cooling overview website (Sept. 25, 2017 at 2:22 p.m. MDT). Data shown in SI units: https://hpc.nrel.gov/COOL/index.html